BBA - Biomembranes 1863 (2021) 183679

Contents lists available at ScienceDirect

BBA - Biomembranes

journal homepage: www.elsevier.com/locate/bbamem

Extracellular ATP hydrolysis in Caco-2 human intestinal cell line

J. Schachter [a,*], C.L. Alvarez [a,b], Z. Bazzi [a], M.P. Faillace [g,h], G. Corradi [a,b], C. Hattab [c,d], D. E. Rinaldi [a,b], R. Gonzalez-Lebrero [a,b], M. Pucci Molineris [e,f], J. Sévigny [i,j], M.A. Ostuni [c,d], P. J. Schwarzbaum [a,b,**]

[a] Instituto de Química y Físico-Química Biológicas "Prof. Alejandro C. Paladini", Universidad de Buenos Aires (UBA), Consejo Nacional de Investigaciones Científicas y Técnicas (CONICET), Facultad de Farmacia y Bioquímica, Junín 956, C1113AAD Buenos Aires, Argentina
[b] Universidad de Buenos Aires (UBA), Facultad de Farmacia y Bioquímica, Departamento de Química Biológica, Cátedra de Química Biológica, Junín 956, C1113AAD Buenos Aires, Argentina
[c] Université de Paris, UMR_S1134, BIGR, Inserm, F-75015 Paris, France
[d] Institut National de la Transfusion Sanguine, Laboratoire d'Excellence GR-Ex, F-75015 Paris, France
[e] Instituto de Investigaciones Bioquímicas de La Plata (INIBIOLP) "Prof. Dr. Rodolfo R. Brenner", Universidad Nacional de La Plata, Consejo Nacional de Investigaciones Cientfficas y Técnicas (CONICET), Facultad de Ciencias Médicas, Av. 60 y Av. 120, La Plata, Argentina
[f] Universidad Nacional de La Plata, Facultad de Ciencias Médicas, Av. 60 y Av. 120, La Plata, Argentina
[g] Instituto de Fisiología y Biofísica Prof. Bernardo Houssay (IFIBIO-Houssay), Universidad de Buenos Aires (UBA), Consejo Nacional de Investigaciones Científicas y Técnicas (CONICET), Buenos Aires, Argentina
[h] Departamento de Fisiología, Facultad de Medicina, Universidad de Buenos Aires (UBA), Buenos Aires, Argentina
[i] Centre de Recherche du CHU de Québec–Université Laval, Québec, QC, Canada
[j] Département de Microbiologie-Infectiologie et d'Immunologie, Faculté de Médecine, Université Laval, Québec, QC, Canada

ARTICLE INFO

Keywords:
Extracellular ATP
ectoATPase
Ectonucleotidases
Purinergic signaling
ATP release
Intestinal epithelial cell

ABSTRACT

Extracellular nucleotides and nucleosides activate signaling pathways that play major roles in the physiology and pathophysiology of the gastrointestinal tract. Ectonucleotidases hydrolyze extracellular nucleotides and thus regulate ligand exposure to purinergic receptors. In this study, we investigated the expression, localization and activities of ectonucleotidases using Caco-2 cells, a model of human intestinal epithelial cells. In addition, by studying ATP release and the rates of extracellular ATP (eATP) hydrolysis, we analyzed the contribution of these processes to the regulation of eATP in these cells. Results show that Caco-2 cells regulate the metabolism of eATP and by-products by ecto-nucleoside triphosphate diphosphohydrolase-1 and -2, a neutral ecto-phosphatase and ecto-5′-nucleotidase. All these ectoenzymes were kinetically characterized using intact cells, and their presence confirmed by denatured and native gels, western blot and cytoimmunofluorescence techniques.

In addition, regulation of eATP was studied by monitoring the dynamic balance between intracellular ATP release and ectoATPase activity. Following mechanical and hypotonic stimuli, Caco-2 cells triggered a strong but transient release of intracellular ATP, with almost no energy cost, leading to a steep increase of eATP concentration, which was later reduced by ectoATPase activity. A data-driven algorithm allowed quantifying and predicting the rates of ATP release and ATP consumption contributing to the dynamic accumulation of ATP at the cell surface.

Abbreviations: 5′NT, Ecto-5′-nucleotidase; ALP, Ecto-alkaline phosphatase; eATP, Extracellular ATP; iPPase, Inorganic pyrophosphatase; NTPDase, Ecto-nucleoside triphosphate diphosphohydrolase; NPPase, Ecto-nucleotide pyrophosphatases/phosphodiesterase; Pi, Inorganic phosphate; POM-1, Polyoxotungstate-1; PPi, Inorganic pyrophosphate; P receptors, Purinergic receptors.

* Corresponding author.
** Correspondence to: P.J. Schwarzbaum, Universidad de Buenos Aires (UBA), Facultad de Farmacia y Bioquímica, Departamento de Química Biológica, Cátedra de Química Biológica, Junín 956, C1113AAD Buenos Aires, Argentina.
E-mail addresses: jschachter@qb.ffyb.uba.ar (J. Schachter), pjs@qb.ffyb.uba.ar (P.J. Schwarzbaum).

https://doi.org/10.1016/j.bbamem.2021.183679
Received 29 March 2021; Received in revised form 8 June 2021; Accepted 10 June 2021
Available online 1 July 2021

1. Introduction

Extracellular nucleotides and nucleosides are autocrine and paracrine signaling molecules that act within tissues to control cell functions. Most of these nucleotides are released in a regulated manner, followed by extracellular conversion to other nucleotides. Stimuli promoting ATP exit include mechanical stress [1,2], hypoxia [3], pathogens [4,5] or exposure to a hypotonic shock [6–8].

In the intestinal epithelium, extracellular ATP (eATP) plays a prominent role modulating the secretion and absorption of ions, uptake of amino acids and sugar transport [9–13]. Upon release, eATP and other nucleotides exert their action through the activation of subtype 2 of purinergic (P) receptors, i.e., ionotropic P2X and metabotropic G protein-coupled P2Y receptors [14]. Whereas P2X receptors respond only to ATP [14], P2Y receptors can be activated by ATP, ADP, UTP, UDP, ITP and nucleotide sugars [15]. Extracellular adenosine (ADO), on the other hand, activates a separate family of P1 receptors [16,17]. Activation of P1 and P2 receptors mediates a wide variety of cellular and physiological effects [18]. In the gastrointestinal system, they are involved in death of human intestinal epithelial cells and immune cell activation, causing several gut pathological conditions [19,20], such as inflammatory bowel disease [21].

Purinergic signaling is critically regulated by enzymes known as ectonucleotidases, which degrade di- and triphosphate nucleotides to their respective nucleosides, thereby controlling the concentration of P2 and P1 agonists on the cell surface [22]. Ectonucleotidases are cell membrane bound enzymes usually displaying their active site to the extracellular milieu, though cleaved and soluble extracellular isoforms may exist [23].

The currently known ectonucleotidases include ecto-nucleoside triphosphate diphosphohydrolases (NTPDases), ecto-nucleotide pyrophosphatases/phosphodiesterases (NPPases), ecto-alkaline phosphatases (ALPs) and ecto-5′-nucleotidases (5′NTs) [23]. There are currently 8 members of the NTPDases family, of which subtypes 1, 2, 3 and 8 are expressed as membrane bound ectoenzymes. NTPDases differ in the specific preference for nucleotides, with K_m values in the low μM range [24]. NTPDase1 hydrolyzes ATP and ADP with approximately similar rates, whereas NTPDase3 and NTPDase8 reveal a preference for ATP over ADP as substrate. NTPDase2, on the other hand, exhibits high ATPase and low ADPase activities [25]. Members of the NPPase family include seven paralogs in mammals (NPP1–7) [23]; they hydrolyze 5′-phosphodiester bonds in nucleotides and their derivatives, producing AMP plus the remaining part, such as inorganic pyrophosphate (PPi) in the presence of the substrate ATP [26].

ALPs are glycosylphosphatidylinositol membrane anchored enzymes known to catalyze the hydrolytic removal of inorganic phosphate (Pi) from a variety of molecules such as lipopolysaccharide, flagellin, CpG DNA, nucleotide di- and tri-phosphates and PPi [27]. In humans, there are 4 different ALP subtypes with different tissue distribution, with intestinal ALP exhibiting a more restricted tissue location [23]. ALPs are the only ectoenzymes capable of fully dephosphorylating ATP to ADO, though a similar hydrolytic conversion was reported to occur by the combined action of NTPDases, NPPases and 5′NT [23]. Thus, the specific set of functional ectonucleotidases expressed in a given tissue and metabolic condition will determine the effective concentration of extracellular nucleotides and nucleosides available at the cell surface for P receptors activation. The contribution of each ectonucleotidase enzymatic family to the eATP hydrolysis in human intestinal cells has not been studied systematically.

In the present study, we used the human colorectal adenocarcinoma Caco-2 cell line to investigate the presence, location, activity and cellular role of ectonucleotidases involved in the hydrolysis of eATP and metabolic byproducts. Caco-2 cells represent a model cell line that phenotypically and morphologically resembles the enterocytes lining the small intestine, and express most P2 receptors identified in human tissues [10,28]. To quantify the contribution of ectonucleotidases to the dynamic cell regulation of eATP, all measurements of enzyme activities were carried out in intact, viable cells.

Results show that Caco-2 cells regulated eATP metabolism by the dynamic interaction between a specific set of ectonucleotidases and non-lytic release of endogenous ATP.

2. Material and methods

2.1. Chemicals

All reagents were of analytical grade. Bovine serum albumin (BSA), paraformaldehyde, Tween-20, polyoxotungstate-1 (POM-1), malachite green, adenosine 5′-triphosphate (ATP), adenosine 5′-diphosphate (ADP), adenosine 5′-monophosphate (AMP), phosphate-buffered saline (PBS), 4-(2-hydroxyethyl)-1-piperazineetahnesulfonic acid (HEPES), ammonium molybdate, *para*-Nitrophenylphosphate (pNPP), Triton X-100, phenylethylsulfonyl fluoride (PMSF) and sodium pyrophosphate were purchased from Sigma-Aldrich (St Louis, MO, USA). D-luciferin was purchased from Molecular Probes Inc. (Eugene, OR, USA). Normal goat serum (NGS) was from Natocor (Cordoba, Cordoba, Argentina). [γ-^{32}P]ATP and [α-^{32}P]ATP were purchased from Perkin Elmer Life Science (Santa Clara, CA, USA).

2.2. Cell culture

Caco-2 cells (ATCC, Molsheim, France) were grown in Dulbecco's modified Eagle's medium (DMEM-F12, Gibco, Grad Island, NY, USA) containing 4.5 g/L glucose (Sigma-Aldrich, St Louis, MO, USA) supplemented with 10% v/v fetal bovine serum, 2 mM L-glutamine (Sigma-Aldrich, St Louis, MO, USA), 100 U/mL penicillin, 100 μg/mL streptomycin and 0.25 μg/mL fungizone (Invitrogen, Carlsbad, CA, USA) in a humidified atmosphere of 5% CO_2 at 37 °C. For ATP kinetics measurements cells were directly seeded on glass coverslips. For ectonucleotidase activity experiments, cells were seeded in cell culture 24-well plates (Corning Costar, NY, USA).

2.3. Solutions

We used two different isotonic media (300 mOsm), either with or without inorganic phosphate (Pi), as follows. Medium with Pi (in mM): 137 NaCl, 2.7 mM KCl, 1 $CaCl_2$, 1 $MgCl_2$, 1. 5 KH_2PO_4, 8 Na_2HPO_4-$7H_2O$, at pH 7.4. Medium without Pi (in mM): 145 NaCl, 5 KCl, 1 $CaCl_2$, 10 HEPES, and 1 $MgCl_2$ at pH 7.4.

Hypotonic solutions were similar in composition as that for isotonic media, except that NaCl was reduced to obtain a final osmolarity of 180 mOsm.

The osmolarity of all media was measured with a vapor pressure osmometer (5100B, Lugan, USA).

2.4. Ectonucleotidase assays

Hydrolysis rates of ATP and other nucleotides were determined by the malachite green assay. In addition, the rate of ATP hydrolysis was also determined by a radioactive method.

2.4.1. Malachite green assay

Ectonucleotidase activity was determined by measuring the amount of free Pi from different nucleotide substrates (adapted from [29]). Caco-2 cells (1.5×10^5 cells) were seeded in 24 wells culture. Before the experiment, cells were washed with the reaction medium lacking Pi. The reaction was initiated by adding 500 μM of each nucleotide substrate (ATP, ADP, AMP) to the reaction medium. At different times, 100 μL of reaction medium were placed in a tube containing 1 mL of cold 25% charcoal in 0.1 M HCl. The tubes were centrifuged at 1500 ×*g* for 10 min. Aliquots (50 μL) of the supernatants containing the released Pi were quantified using the malachite green colorimetric reagent. A calibration

curve was run using assay medium containing different concentrations of Pi. The malachite green reagent was prepared by mixing 2 g of sodium molybdate, 0.3 g of malachite green, and 0.5 g of Triton X-100 in 1 L of 0.7 M HCl. Non-enzymatic Pi release was determined by running similar experiments in the absence of cells, whereas initial Pi contents were determined in the absence of substrates which were added after the reaction was stopped. Non enzymatic nucleotide hydrolysis was negligible.

2.4.2. Radioactive assay

The rate of eATP hydrolysis was determined by following the accumulation of [^{32}P]Pi release from exogenous [γ-^{32}P]ATP to Caco-2 cells (1.5×10^5 cells) attached to a 24 wells plate, as described before [30]. Cells were taken from culture and washed with media with or without Pi. The reaction was started by adding [γ-^{32}P]ATP (120 Ci/mmol, 4, 8, 12 or 500 μM) to adhered cells at room temperature and was stopped at the indicated time periods by adding 750 μL of a stop solution containing 4.05 mM $(NH_4)_6Mo_7O_{24}$ and 0.83 mM $HClO_4$. The ammonium molybdate solution formed a complex with the released Pi, which was then extracted with 0.6 mL of isobutyl alcohol. Phases were separated by centrifugation at 1000 $\times g$ for 3 min, aliquots of 200 μL of the organic phase containing [^{32}P]Pi were transferred to vials with 2 mL of 0.5 M NaOH and radioactivity was measured by the Cerenkov effect. Initial [^{32}P]Pi concentrations were measured in assay media without cells. The [^{32}Pi] mass produced from [γ-^{32}P]ATP was calculated using the [γ-^{32}P]ATP specific activity.

For both methods, nucleotidase activity was calculated by fitting the following exponential function to data:

$$Y = Y_0 + A\cdot\left(1\text{–}exp^{-k\cdot t}\right)$$

where Y and Y_0 are the values of [Pi] at each time (t) and at $t = 0$, respectively; A represents the maximal value for the increase in Y with time and k is a rate coefficient. The parameters of best fit resulting from the regression were used to calculate the initial rate of nucleotidase activity (v_i) as $k \times A$.

In experiments of Fig. 9, production of ADO from ATP was estimated at room temperature by following the release of [^{32}P]Pi from [α-^{32}P]ATP in Caco-2 cells. Methods and mathematical analysis were similar to those described for detecting [^{32}P]Pi release from exogenous [γ-^{32}P]ATP. Using [α-^{32}P]ATP, one ADO is formed for every [^{32}P]Pi produced.

2.5. Antibodies

All the primary antibodies used in this study have been previously characterized and validated. The following primary antibodies were used for immunocytochemistry: rabbit polyclonal anti-human NTPDase1 (hN1-S_L) [31], mouse monoclonal anti-human NTPDase2 (hN2-H9$_s$) [32], and rabbit polyclonal anti-human ecto-5′-nucleotidase (h5′NT-2$_L$I$_5$) [31]. Goat polyclonal anti-mouse or anti-rabbit Cy3-conjugated secondary antibodies were obtained from Jackson ImmunoResearch Laboratories (West Grove, PA, USA). The following primary antibodies were used for Western blotting: polyclonal guinea pig anti-human NTPDase1 (hN1-1$_C$I$_5$) [31], mouse monoclonal anti-human NTPDase2 (hN2-H9$_s$), rabbit polyclonal anti-human ecto-5′-nucleotidase (h5′NT-2$_L$I$_5$): mouse monoclonal anti-human NTPDase3 (hN3-B3$_s$) [33] and mouse monoclonal anti-human NTPDase8 (hN8-D7A$_s$) [34].

2.6. Western blots

Caco-2 cells were cultured in 75 cm^2 culture flasks up to 50% of confluence before being harvested through treatment with Cell Dissociation Buffer (Thermo Fisher Scientific, Waltham, MA USA) and mechanical dissociation. Cells were then washed in PBS and centrifuged. The resulting pellet was suspended in Lysis Buffer (10 mM Tris-HCl pH 6.8, 1 mM EDTA, 10% SDS, containing 1× cOmplete™ Protease Inhibitor Cocktail, Roche) for 60 min at 4 °C. Protein quantification was performed by Pierce™ BCA Protein Assay Kit (Thermo Fisher Scientific, Waltham, MA, USA) and 35–45 μg of cell lysate were loaded on NuPAGE® 4–12% Bis-Tris gels, as indicated, under nonreducing conditions. Proteins were transfered to a nitrocellulose membrane using Trans-Blot Turbo Transfer System (BioRad, Hercules, CA, USA), followed by immunoblotting by exposure to primary antibody (dilution 1:1000) overnight at 4 °C. Proteins of interest were revealed using HRP-conjugated secondary antibodies and the ECL™ Western Blotting Reagents kit (Merck, GE Healthcare, Chicago, IL, USA). Images were acquired by ChemiDoc™ Imaging Systems (Bio-Rad, Hercules, CA, USA). Pre-immunized serum was used as negative control.

2.7. Immunocytochemistry

Caco-2 cells adhered to glass coverslips were fixed with 4% paraformaldehyde for 10 min at room temperature, washed with PBS and incubated for 30 min at 4 °C with the plasma membrane marker Alexa 488-conjugated wheat germ agglutinin (WGA, Molecular Probes, Eugene, OR, USA). After that period, the cells were washed with PBS-T (PBS plus 0.1% Tween-20) and incubated 2 h with a blocking solution containing 10% of NGS in PBS-T. Then, samples were washed with PBS-T and incubated at 4 °C overnight in a humid chamber with each primary antibody diluted in 5% NGS in PBS-T. Antibodies were diluted as follows: hN1-S_L (1:100); hN2-H9$_s$ (1:50) and h5′NT-1$_L$ (1:50). Coverslips were washed with PBS-T and then incubated in darkness for 2 h at room temperature with secondary antibodies against either mouse or rabbit primary antibodies diluted (1:500) in 3% NGS in PBS-T. Samples were thoroughly washed with PBS-T and incubated 30 min in darkness at room temperature with 5 μg/mL Hoechst. Finally, coverslips were washed with PBS and distilled water and mounted with DABCO (2.5%) in PBS:glycerol (1:9) for fluorescence detection.

Fluorescent cell images were captured with a FV1000 Fluoview confocal spectral microscope (Olympus, Tokyo, Japan) with SAPO-60× oil and numerical aperture of 1.35. Two-dimensional reconstruction was performed with Fluoview Software (Olympus, Tokyo, Japan).

2.8. PPase activity measurement

The production of PPi resulting from eATP hydrolysis by NPPase activity cannot be detected by the malachite green colorimetric assay, which only detects Pi. Thus, NPPase activity of Caco-2 cells was estimated running the malachite green assay (as described in Section 2.4.1) in the presence of 500 μM ATP and 1 U/mL inorganic pyrophosphatase (iPPase, from yeast, Sigma-Aldrich, St Louis, MO, USA). Under this condition, any PPi molecule produced by a putative NPPase will be converted to Pi by iPPase and will be detected by the malachite green assay.

2.9. Hydrolysis of p-nitrophenil phosphate

The extracellular hydrolysis of *p*-nitrophenylphosphate (pNPP) by Caco-2 cells was measured at room temperature by following the release of *p*-nitrophenol from pNPP, as previously described [35]. The reaction was carried out using intact Caco-2 cells in a reaction medium without Pi for 60 min, except when otherwise indicated. The production of *p*-nitrophenol in the supernatants was determined by measuring the optical density at 410 nm. Blanks obtained without cells were subtracted from each experimental data point. A molar extinction coefficient of $1.78 \times 10^4\ M^{-1}\ cm^{-1}$ was used to convert optical density to mass of *p*-nitrophenol released. Results are expressed as pmol of *p*-nitrophenol per μg of protein. Protein contents of each sample were quantified by the Bradford method [36].

As a positive control experiment, a few experiments were run in the absence of cells, but in the presence of a recombinant calf intestinal

alkaline phosphatase (Promega, Madison, WI, USA).

2.10. Detection of pNPPase activity in gels

The samples of Caco-2 lysates were electrophoresed under denaturing conditions in 9% polyacrylamide gels (SDS-PAGE) as described previously [37]. Gels were washed twice with distilled water for 10 min to remove SDS and incubated 20 min under gentle stirring in the presence of 10 mL of assay medium without Pi containing 12 mM of pNPP. Gels were then washed twice with 100 mL water to remove substrate excess, and phosphatase activity was detected as a yellow band corresponding to *p*-nitrophenol production.

2.11. Extracellular ATP measurements

The eATP concentration ([eATP]) of intact Caco-2 cells was measured using the firefly luciferase reaction (EC 1.13.12.7, Sigma-Aldrich, St Louis, MO, USA), which catalyzes the oxidation of D-luciferin in the presence of ATP to produce light [38]. Measurements were performed with cells seeded on coverslips that were mounted in the assay chamber of a custom-built luminometer, as previously described [39]. Because luciferase activity at 37 °C is only 10% of that observed at 20 °C [40], to maintain full luciferase activity, [eATP] measurements were performed at room temperature.

The setup allowed continuous measurements of eATP to be taken via the light output detection of the luciferin-luciferase reaction. The time course of light emission was transformed into [eATP] versus time by means of a calibration curve. Increasing concentrations of ATP from 20 to 1000 nM were sequentially added to the assay medium from a stock solution of pure ATP dissolved in isosmotic or hypotonic medium, according to the experiment. Calibration curves displayed a linear relationship within the range tested. Results were expressed as [eATP] at every time point of a kinetics curve denoted as "eATP kinetics", with [eATP] expressed as pmol of ATP/μg protein in a final assay volume of 100 μL. After each experiment, cells were lysed with a solution containing 1 mM PMSF and 0.1% of Triton X-100 and the protein contents of each sample were quantified [36].

2.12. Viability test

The Trypan Blue dye exclusion test was used to determine the number of viable cells in suspensions of Caco-2 cells after being exposed to either isotonic or hypotonic media. Caco-2 cells cultures were treated with Trypsin washed with medium with Pi and counted. Then 1.5×10^5 cells in 1 mL were exposed to isotonic or hypotonic media for 30 min, after which Trypan Blue was added to the cell suspension (final concentration 0.4 mM) under mixing, and the number of non-viable cells (blue cells) was counted a Neubauer chamber. The percentage of viable cells was calculated as:

$$\%\text{viable cells} = [1\text{–}(\text{number of blue cells}/\text{number of total cells})] \times 100$$

2.13. Predictions of eATP kinetics

In Fig. 11, a theoretical curve was built where the effect of eATP hydrolysis on eATP kinetics was subtracted. That is, the linear equation describing ectoATPase activity vs [ATP] (derived from data of Fig. 8) was used to calculate eATP consumption at every time point of the eATP kinetics curve (data of Fig. 10). Then, values of eATP consumption obtained were used to calculate the accumulated [eATP] consumed during eATP kinetics, thus generating an ectoATPase curve. Then, by subtracting the contribution of this ectoATPase curve to the experimental eATP kinetics, a "predicted eATP kinetics" was calculated where the effects of ectoATPase activity were mathematically eliminated. All results were expressed as nM/well. Finally, the predicted eATP efflux (nM/min) was calculated by numerical differentiation of the predicted eATP kinetics.

2.14. Data analysis

Statistical significance was determined using ANOVA and Bonferroni test for a posteriori comparison or the non-parametric Mann-Whitney test. Data were analyzed and graphically represented using GraphPad Prism software v5.0 (Graph Pad Software, San Diego, CA, USA).

3. Results

3.1. Ectonucleotidase activities in Caco-2 cells

Several ectoenzymes are able to hydrolyze eATP and by-products. At relative high concentrations of these nucleotides, ectonucleotidase activities estimate the apparent maximal rates of hydrolysis ($appV_{max}$). Accordingly, we used the malachite green assay to assess the time course of Pi accumulation in the presence of 500 μM of ATP, ADP or AMP (Fig. 1A), and calculated $appV_{max}$ values for each substrate using intact Caco-2 (Fig. 1B). The highest $appV_{max}$ value amounted to 43.1 ± 3.8 pmol/μg protein/min in the presence of ATP. When AMP was used as substrate, $appV_{max}$ value was significantly lower (48% of ectoATPase activity), whereas using ADP $appV_{max}$ value was only 8% of ectoATPase activity.

We further evaluated the effect of polyoxotungstate (POM-1), an inhibitor of NTPDase1–3 [41], on ectonucleotidase activity of Caco-2 cells. Cells were pre-incubated for 15 min with either 10 or 100 μM POM-1 before addition of substrates (500 μM of ATP or AMP), and the indicated concentration of inhibitor was maintained during the course of the reaction. As expected, POM-1 displayed a dose-dependent inhibition of ectonucleotidases activities in Caco-2 cells (Fig. 1C). That is, ectoATPase activity was inhibited 48% by 10 μM POM-1 and 92% by 100 μM POM-1, while ectoAMPase activity was inhibited 52% by 100 μM POM-1, with no significant effects being observed using 10 μM of the inhibitor.

3.2. Localization of NTPDase1, NTPDase2 and 5′NT in Caco-2 cells

We performed western blot analysis and immunofluorescence confocal microscopy to identify the ectonucleotidases responsible for the observed hydrolytic activities of extracellular nucleotides. For western blot, samples were prepared from Caco2- cells lysates. Specific antibodies against human NTPDase1, -2, -3, -8 and 5′NT were used.

NTPDase1 and -2 were identified as ~77 kDa and ~ 61 kDa bands, respectively. Immune reactive bands for NTPDase3 and -8 were not observed. 5′NT was identified by a ~ 47 kDa band (Fig. 2). No bands were recognized by equal dilution of pre-immunized serum from rabbit and guinea pig used to respectively produce polyclonal antibodies against 5′NT and NTPDase1 (data not shown).

Immunofluorescence confocal microscopy images of Caco-2 cells confirmed the expression of NTPDase1, NTPDase2 and 5′NT (Fig. 3A, E and I). To gain further insight in the subcellular localization of ectonucleotidases, Caco-2 cells were co-stained with the nuclei marker Hoechst (Fig. 3B, F and J, blue label) and the fluorescent marker of glycosylated surface-expressed proteins Alexa Fluor 488-WGA (Fig. 3C, G and K, green label). Merge of single plane confocal images showed an overlap of NTPDase1, NTPDase2 and 5′NT with the plasma membrane (orange signal in Fig. 3D, H and L).

3.3. Potential contribution of NPPases to the ectoATPase activity of Caco-2 cells

Up to here, results showed that Caco-2 cells displayed active ectoATPase, ectoADPase and ectoAMPase activities which can, in principle, be assigned to NTPDases1 and -2, and 5′NT. However, our methods used to assess nucleotide hydrolysis detect only release of Pi,

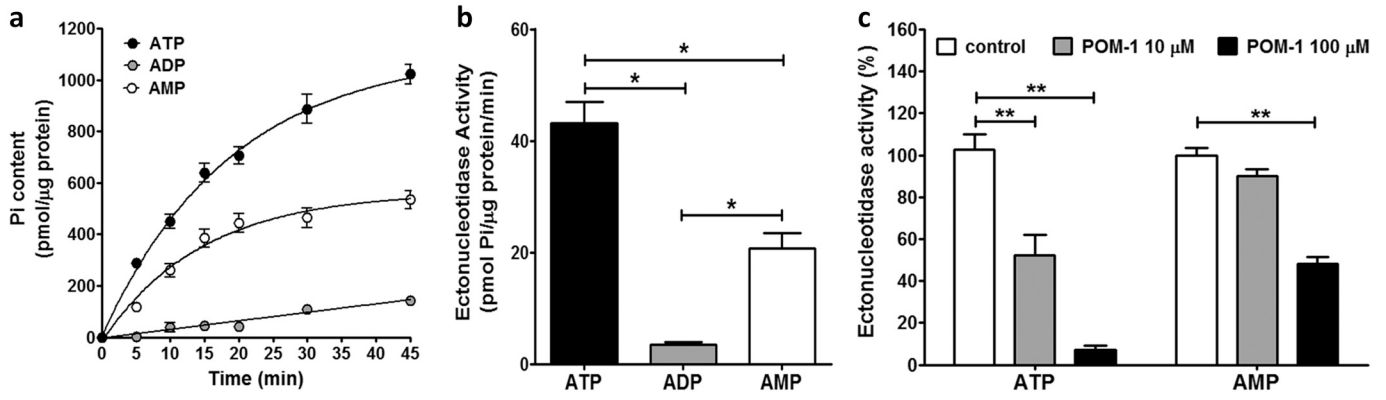

Fig. 1. Ectonucleotidase activity of Caco-2 cells using different nucleotides as substrates.
Experiments were performed in assay medium without Pi at room temperature, and Pi production was measured by the malachite green method. (A) Time course of Pi accumulation in supernatants of Caco-2 cells incubated with 500 µM of ATP (black), ADP (grey) or AMP (white). The continuous lines represent the fitting of monoexponential functions to experimental data. Results are expressed as pmol Pi/µg protein and are means ± s.e.m. $N = 14$ independent experiments run in duplicate. (B) Values of apparent Vmax ($appV_{max}$) were derived from initial rates of the monoexponential functions fitted to data of (A). Results are expressed as pmol Pi/µg protein/min and are means ± s.e.m. * denote $p \leq 0.05$, ANOVA and a posteriori Bonferroni multiple comparison test. (C) Effect of POM-1 on normalized $appV_{max}$ values of nucleotidase activities in Caco-2 cells. Cells were pre-treated 30 min with 0 (white, control), 10 µM (grey) and 100 µM (black) POM-1. Subsequently, cells were incubated in assay media in the absence or presence of POM-1 and in the presence of 500 µM of either ATP or AMP. Results are means ± s.e.m. and are expressed as the percentage of the ectonucleotidase activity obtained in the absence of POM-1 for each substrate, at 10 min. $N = 4$ independent experiments run in duplicate. ** denote $p < 0.01$, Mann-Whitney test. (For interpretation of the references to color in this figure legend, the reader is referred to the web version of this article.)

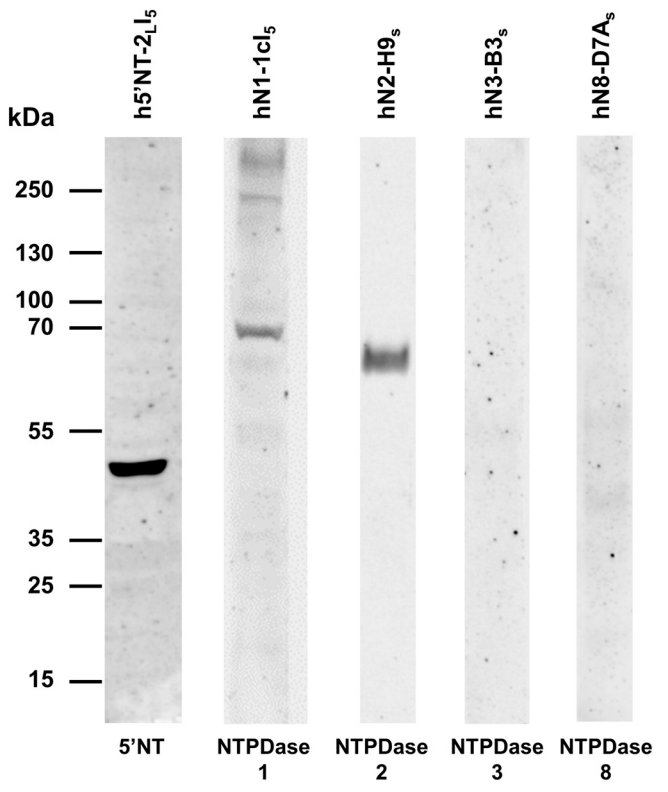

Fig. 2. Western blots of 5′NT and NTPDases isoforms -1,-2,-3 and-8 in Caco-2 cell lysates.
Samples of whole Caco-2 cell lysates were immunoblotted using different nucleotidases antibodies (dilution 1/1000): rabbit polyclonal anti-human 5′NT, guinea pig polyclonal anti-human NTPDase1, and mouse monoclonal antibodies anti-human NTPDase2, NTPDase3 and NTPDase8, as indicated. Membranes were revealed using HRP-conjugated secondary antibodies. Images are representative of 4 independent experiments.

and are therefore unable to detect a potential degradation of eATP directly into AMP plus PPi. Such additional eATP degradation may occur if functional ectophosphodiesterases of the NPP family were present in Caco-2 cells.

Accordingly, NPPase activity was estimated in the presence of 500 µM ATP and 1 U/mL inorganic pyrophosphatase (iPPase). Under this condition, any PPi produced by a putative NPPase will be converted to Pi by the iPPase and will be detected by the malachite green assay. Results showed no difference in ectoATPase activity in the presence or absence of iPPase (Fig. 4A), indicating that, under our experimental conditions, there was no contribution of PPase activity to eATP hydrolysis of Caco-2 cells.

We also tested the potential presence of ectopyrophosphatase activity in Caco-2 cells by using PPi as a substrate. Addition of 50 µM PPi in a Pi free assay medium containing Caco-2 cells during 45 min did not generate measurable amounts of Pi, thus discarding a contribution of NPPase activity to eATP hydrolysis of Caco-2 cells. To validate the procedure, we verified pyrophosphatase activity of pure iPPase in the absence of cells. Results showed that iPPase was able to hydrolyze 10 or 50 µM PPi after 10 or 40 min (Fig. 4B).

3.4. Contribution of ectophosphatases to eATP hydrolysis of Caco-2 cells

Having discarded the contribution of NPPases to eATP hydrolysis, we turned our attention to ectophosphatases. Expression of an intestinal ALP has been reported before [42,43]. First, we run experiments aimed at testing the capacity of intact Caco-2 cells to hydrolyze pNPP, a substrate for phosphatases, but not for NTPDases or 5′NT.

As shown in Fig. 5A, Caco-2 cells exhibited ectophosphatase activity and this activity increased with [pNPP] in a hyperbolic pattern, with $K_{0.5\ pNPP} = 1056 \pm 101$ µM and $appV_{max}$ 1.30 ± 0.07 pmol *p*-nitrophenol/µg protein/min. The presence of ectophosphatase activity in Caco-2 cells was further corroborated by using denaturing gel electrophoresis, where a broad band of *p*-nitrophenol accumulation was identified. This band is roughly similar to that formed by the activity of the recombinant calf intestinal alkaline phosphatase used as positive control (Fig. 5B).

Ammonium molybdate (1 mM), a potent inhibitor of phosphatases [44], strongly inhibited pNPP hydrolysis (Fig. 5A), causing a 102% increase of $K_{0.5\ pNPP}$ ($K_{0.5\ pNPP} = 2140 \pm 262$ µM) and a 79% reduction of

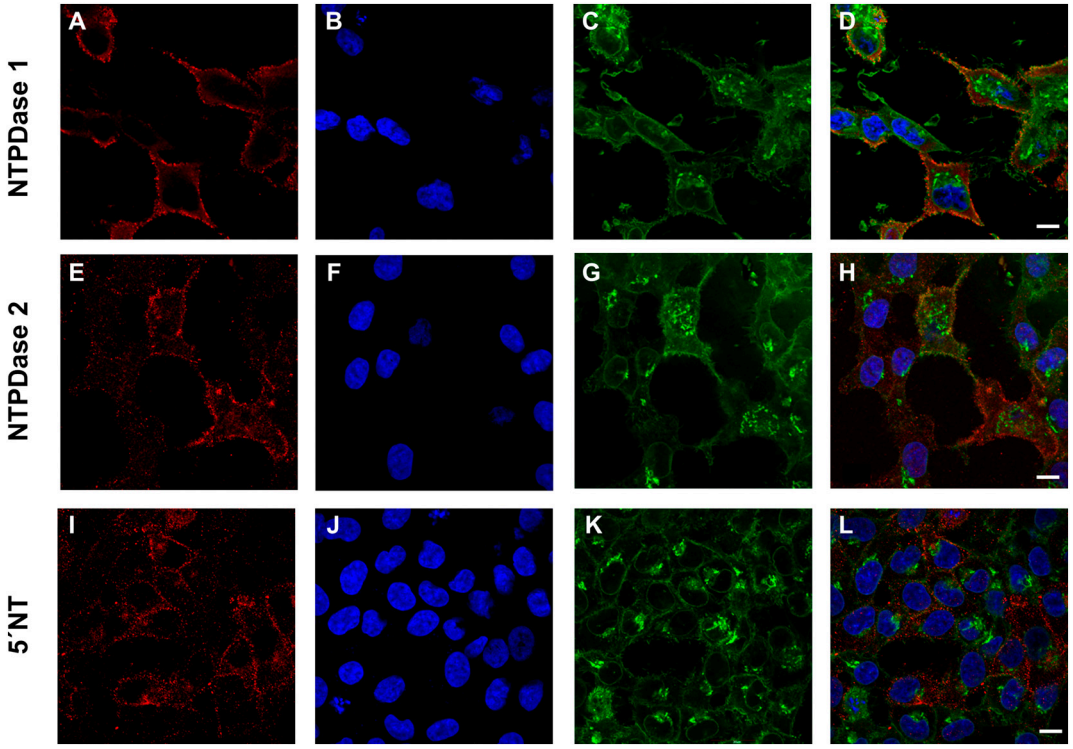

Fig. 3. Detection and localization of NTPDases in Caco-2 cells.
Confocal microscopy images of immunofluorescence experiments performed in Caco-2 cells using primary antibodies against human NTPDase1 (A–D), human NTPDase2 (E–H) and human 5′NT (I–L), together with a secondary Cy3-conjugated antibody (red, A, E and I). In all experiments, cells nuclei were labeled with Hoechst (blue, B, F and J), and plasma membranes with 488-conjugated WGA (green, C, G and K). Individual immunoreactivity of each ectonucleotidase in A (NTPDase1), E (NTPDase2) and I (5′NT antibody); merged images of NTPDase1 (D), NTPDase2 (H) and 5′NT (L) with Hoechst and WGA. Scale bars: 10 μm. $N = 3$ independent experiments. (For interpretation of the references to color in this figure legend, the reader is referred to the web version of this article.)

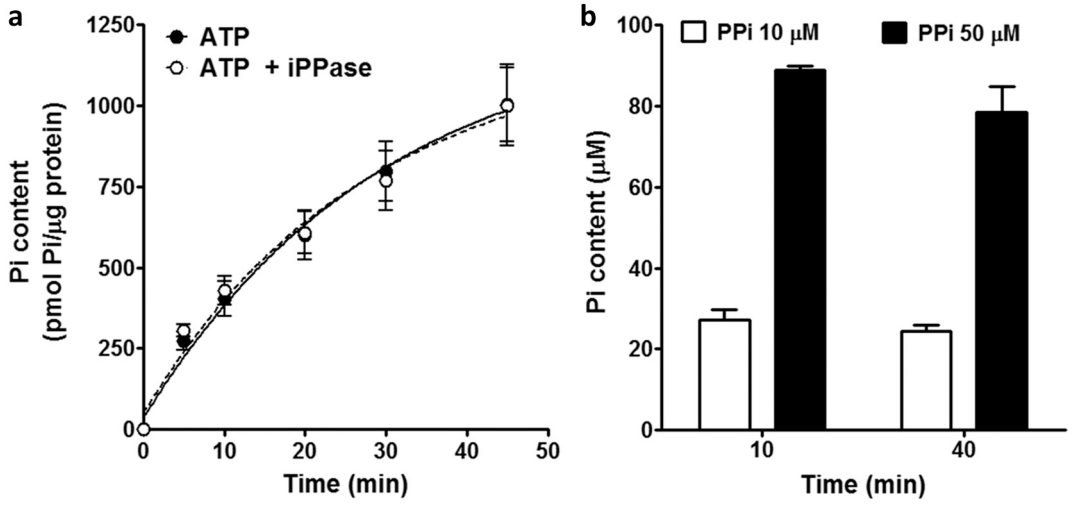

Fig. 4. Ectonucleotide pyrophosphatase/phosphodiesterase activity in Caco-2 cells.
(A) Time course of Pi accumulation in supernatants of Caco-2 cells incubated with 500 μM of ATP in the absence (black, continuous line) or in the presence of 1 U/mL of inorganic pyrophosphatase (iPPase) (white, dashed line). Experiments were performed in assay medium without Pi at room temperature and the Pi concentration was measured by the malachite green method. Lines represent the fitting of exponential functions to experimental data. Results are expressed as means ± s.e.m., $N =$ 4 independent experiments run in duplicate. (B) 10 μM (white) or 50 μM (black) of sodium PPi were diluted in 300 μL of a reaction medium without Pi, and 1 U/mL of inorganic pyrophosphatase (iPPase) was added. The reaction was performed at room temperature and after 10 or 40 min the Pi content (μM) in the medium was measured by the malachite green assay. Results are means ± s.e.m. of one experiment done in triplicate. (For interpretation of the references to color in this figure legend, the reader is referred to the web version of this article.)

$appV_{max}$ ($appV_{max} = 0.274 \pm 0.05$ pmol *p*-nitrophenol/μg protein/min). On the other hand, POM-1 showed a different inhibitory effect on ectophosphatase activity (Fig. 5C), in that $K_{0.5\ pNPP}$ values increased by 73% ($K_{0.5\ pNPP} = 1830 \pm 418$ μM), while $appV_{max}$ was not altered ($appV_{max} = 1.36 \pm 0.1$ pmol product/μg protein/min).

By testing the pH dependence, we observed that ectophosphatase

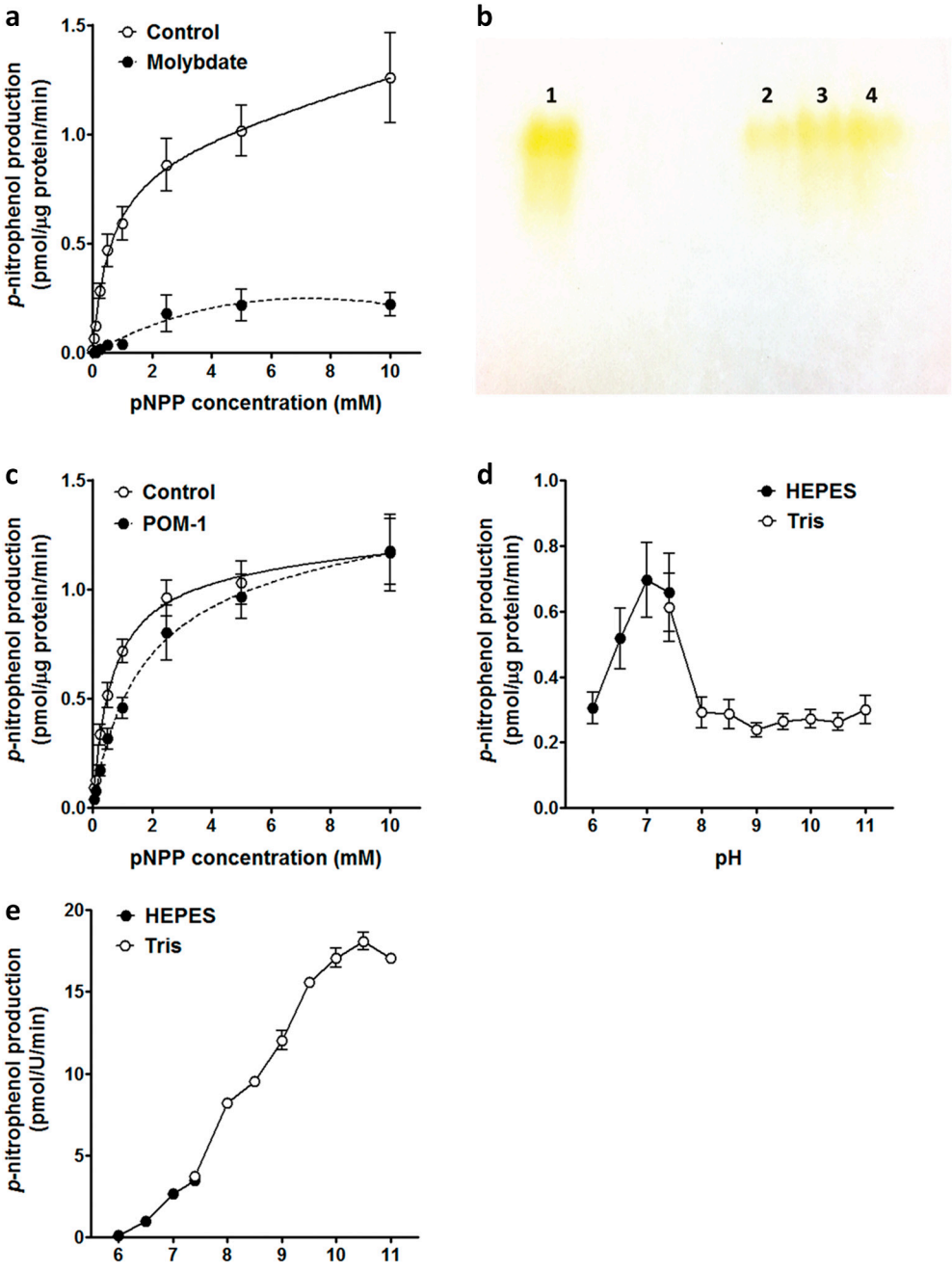

Fig. 5. Ectophosphatase activity in Caco-2 cells.
Ectophosphatase activity in Caco-2 cells was estimated by the release of *p*-nitrophenol from pNPP. (A and C) Cells were incubated for 60 min at room temperature with increasing concentrations of pNPP (0.01–10 mM) at pH 7.4 in assay media lacking Pi. Experiments were run in the absence of inhibitors (white symbol and continuous line, control), in the presence of 1 mM ammonium molybdate (black symbol and dotted line in A, $N = 4$ independent experiments run in duplicate) or in the presence of 100 µM POM-1 (black symbol and dotted line in C, $N = 3$ independent experiments run in duplicate). (B) Samples of protein extracts from Caco-2 cells were run on SDS-PAGE gels. Phosphatase activity was detected by the presence of a yellow band corresponding to *p*-nitrophenol production from pNPP. A positive control was run by following the same procedure in the presence of a recombinant alkaline phosphatase. Lane 1: 0.1 U of recombinant calf intestinal alkaline phosphatase. Amounts of loaded Caco-2 protein extracts were 10 µg (Lane 2), 15 µg (Lane 3) and 20 µg (Lane 4). (D) Cells were incubated for 60 min at room temperature with 1 mM pNPP and the production p-nitrophenol were measured in media at different pH values using a HEPES buffer (pH 6–7.5) and Tris-HCl buffer (pH 7.5–11), N = 3 independent experiments run in duplicate. (E) The phosphatase activity of recombinant calf intestinal alkaline phosphatase (0.1 U/mL) was tested in media without cells, by incubating the enzyme for 6 min at room temperature with 250 µM pNPP. Media at different pHs were similar as in D, $N = 1$ experiment done in triplicate. (A, C–E) Results are expressed as means ± s.e.m. (For interpretation of the references to color in this figure legend, the reader is referred to the web version of this article.)

activity in Caco-2 reached a maximum at pH 7–7.5 (Fig. 5D). Under similar conditions, the recombinant phosphatase – in the absence of cells - showed a maximal activity at pH 10–11, as previously described (Fig. 5E) [23]. Thus, a neutral ectophosphatase activity seems to be functional in Caco-2 cells. To investigate the ability of ectophosphatases present in Caco-2 cells to hydrolyze ATP, ADP and AMP, a displacement experiment testing pNPP hydrolysis in the presence of these nucleotides was performed. Increasing amounts of ATP, ADP and AMP (10–1000 µM) were added to reaction media in the presence of a constant concentration of pNPP (1 mM). Under this condition, 1 mM of ATP, ADP or AMP decreased >85% of *p*-nitrophenol production (Fig. 6), suggesting that ectophosphatase can bind extracellular ATP, ADP and AMP, as well as pNPP, at the catalytic site. Apparent inhibition affinity was the highest with AMP ($K_{0.5} = 16.03 \pm 1.97$ µM), followed by ADP ($K_{0.5} = 65.74 \pm 2.76$ µM) and ATP ($K_{0.5} = 65.74 \pm 2.76$ µM).

Since ectophosphatase activity might contribute to eATP hydrolysis in Caco-2 cells, we next examined the effect of the phosphatase inhibitor ammonium molybdate on ectoATPase activity. Because the ammonium molybdate interferes with the malachite green method, the radioactive method was used. Accordingly, Caco-2 cells were exposed to [γ-^{32}P]ATP at 500 µM ATP and the time course of [^{32}P]Pi accumulation released from [γ-^{32}P]ATP was determined. As shown in Fig. 7A, molybdate did not affect the time course of [γ-^{32}P]ATP hydrolysis.

Colorimetric experiments measuring pNPP hydrolysis required the use of media lacking Pi, while experiments using [γ-^{32}P]ATP were performed in media containing milimolar Pi. Since free Pi may potentially exert product inhibition on ectophosphatase activity, it was interesting to test its effects on the rate of eATP hydrolysis. Using 500 µM ATP, $appV_{max}$ values were 64% higher in the absence of Pi, than in its presence ($appV_{max}$ with Pi = 9.5 ± 0.91 pmol product/µg protein/min vs $appV_{max}$ without Pi = 17.93 ± 1.69 pmol product/µg protein/min) (Fig. 7B).

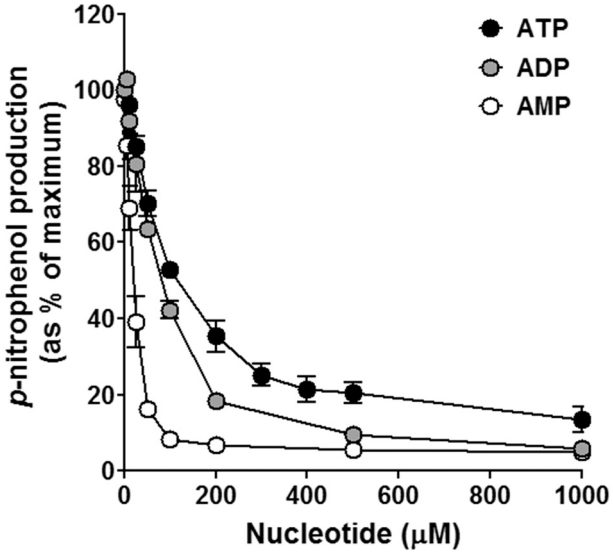

Fig. 6. Effects of AMP, ADP and ATP on pNPP hydrolysis.
Cells were incubated for 60 min at room temperature with 1 mM pNPP, and increasing amounts of AMP, ADP or ATP (0–1 mM) were added. Experiments were run in isotonic medium without Pi, pH 7.4, and the *p*-nitrophenol production was measured. Results are expressed as normalized *p*-nitrophenol production, i.e., the percentage of ectophosphatase activities measured in the absence of nucleotides, and are means ± s.e.m. N = 3 independent experiments run in duplicate.

Taken together, the above results indicate that, in addition to NTPDase1 and -2, eATP can be hydrolyzed by an ectophosphatase present in Caco-2 cells, which exhibits an optimal pH between 7 and 7.5 and is inhibited by both molybdate and Pi.

The following experiments were designed to analyze eATP regulation in a more physiological context. On the one hand, we quantified ectoATPase activity in the low micromolar range of [ATP]. Then, we studied the kinetics of eATP accumulation in the presence of stimuli known to induce ATP release. Finally, since eATP kinetics depends on the balance between ATP release and eATP hydrolysis, we analyzed eATP kinetics and eATP hydrolysis simultaneously by running a small algorithm to predict the contribution of these two processes to eATP regulation of Caco-2 cells.

3.5. NTPDase activity in Caco-2 cells

Caco-2 cells were exposed to [γ-^{32}P]ATP at 4, 8 and 12 μM ATP and the time course of [^{32}P]Pi accumulation released from [γ-^{32}P]ATP was determined (Fig. 8A). EctoATPase activity increased with [ATP] in the reaction media. The initial rate values of [^{32}P]Pi production were used to calculate ectoATPase activity at each [eATP], so as to build a substrate curve. EctoATPase activity followed a linear function with [ATP] from 4 to 12 μM (Fig. 8B), with the slope of the curve (K_{ATP}) amounting to 29.02 ± 0.001 pmol [^{32}P]Pi/mg protein/min/μM.

To test the ability of Caco-2 cells to generate ADO from eATP, we performed an experiment using [α-^{32}P]ATP at 12 μM, where one ADO is formed for every [^{32}P]Pi produced. Accordingly, we measured the time course of [^{32}P]Pi accumulation released from [α-^{32}P]ATP (Fig. 9A) and calculated the percentage of total ATP hydrolyzed at each time point. A comparison of Pi release from [γ-^{32}P]ATP and [α-^{32}P]ATP at 12 μM showed that the hydrolysis rate was 3-fold higher for [γ-^{32}P]ATP than [α-^{32}P]ATP ([γ-^{32}P]ATP = 9 ± 1%ATP hydrolyzed/mg protein/min vs [α-^{32}P]ATP = 3.2 ± 0.4%ATP hydrolyzed/mg protein/min) (Fig. 9B).

We also tested the possibility that Caco-2 cells may release active nucleotidases to culture media, in which case exoATPase activity should be detectable and therefore contribute to eATP hydrolysis. For this purpose, cells were cultured for 3 days, and the culture media was extracted for testing. Exposure of these media to 500 μM [γ-^{32}P]ATP during 120 min produced no detectable [γ-^{32}P]Pi.

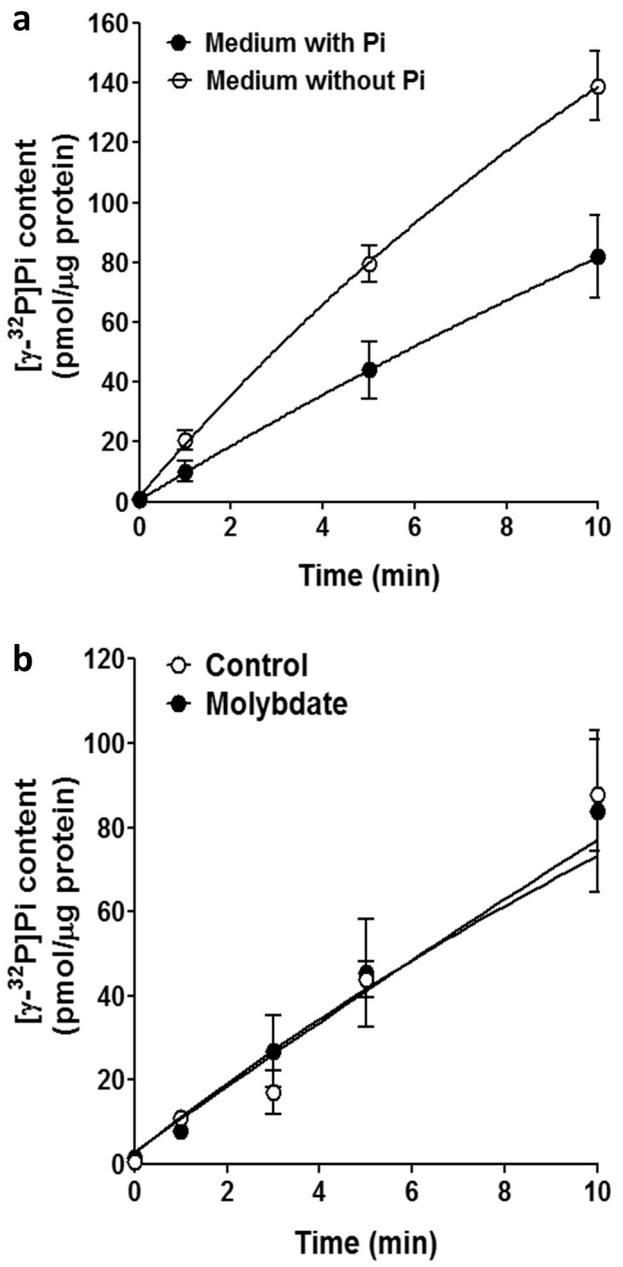

Fig. 7. Effects of ammonium molybdate and inorganic phosphate on ectoATPase activity of Caco-2 cells.
Rates of [^{32}P]Pi accumulation released from exogenous 500 μM [γ-^{32}P] ATP in the supernatants of Caco-2 cells. (A) Cells were incubated in assay medium with Pi in the presence of 1 mM ammonium molybdate (white), or in its absence (black, control), *N* = 4 independent experiments run in duplicate. (B) Cells were incubated in isosmotic medium with Pi (black) or without Pi (white), N = 3 independent experiments run in duplicate. The continuous lines represent the fitting of exponential functions to experimental data. Results are expressed as means ± s.e.m.

3.6. eATP kinetics

Online luminometry was used to study the kinetics of [eATP] accumulation (i.e., eATP kinetics) when Caco-2 cells were stimulated by hypotonicity and mechanical stress. Under unstimulated conditions

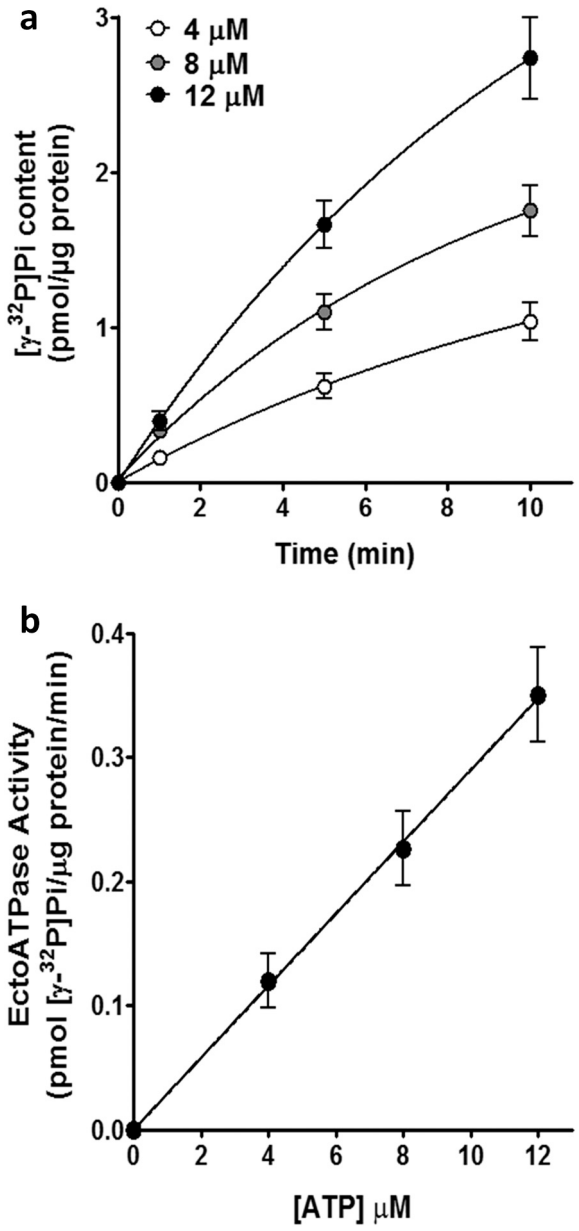

Fig. 8. EctoATPase activity of Caco-2 cells at low eATP concentrations. (A) Time course of [^{32}P]Pi accumulation released from exogenous [γ-^{32}P]ATP (4, 8 and 12 μM) in the supernatants of Caco-2 cells. The reactions were performed in isotonic medium (300 mOsm) containing Pi at room temperature. The continuous lines represent fittings of exponential functions to experimental data for each ATP concentration used (white for 4 μM, grey for 8 μM and black for 12 μM), from which initial rates were calculated (see Materials and Methods). (B) Ecto-ATPase activity as a function of ATP concentration. Each symbol represents ectoATPase activity calculated as the initial rate of Pi production using data from (A). The line represents the fit of a linear function to experimental data. Results are expressed as means ± s.e.m. $N = 8$ independent experiments run in duplicate.

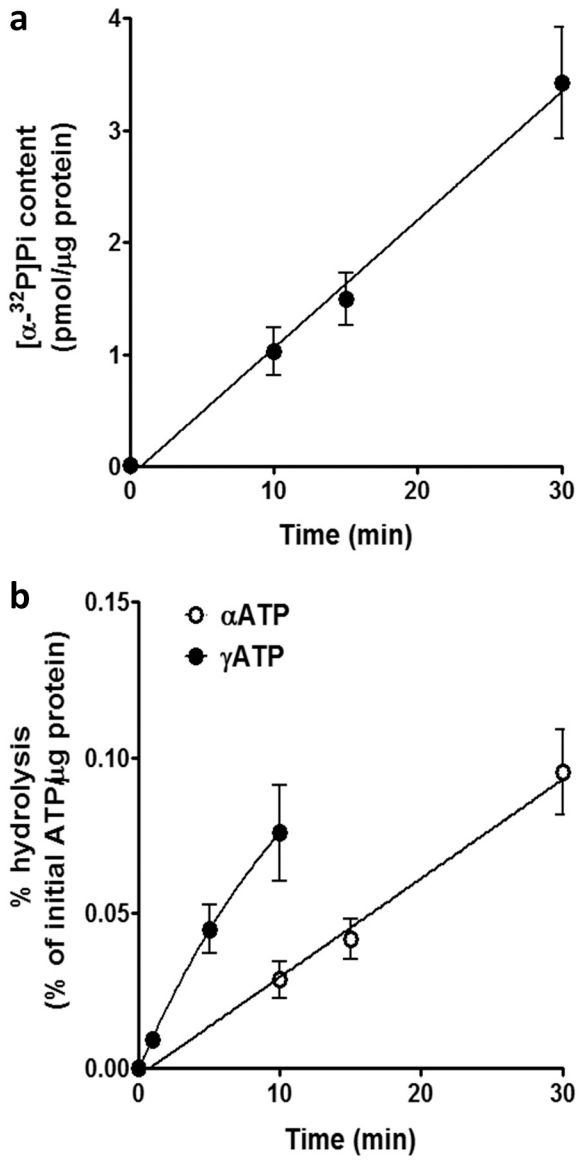

Fig. 9. Adenosine production by eATP hydrolysis in Caco-2 cells. (A) Time course of [^{32}P]Pi accumulation released from [α-^{32}P]ATP (12 μM) in the supernatants of Caco-2 cells. Experiments were performed in isotonic medium with Pi (300 mOsm) at room temperature. The continuous line represents the fitting of an exponential function to experimental data. $N = 4$ independent experiments run in duplicate. Results are expressed as pmol [P^{32}] Pi/μg protein and are means ± s.e.m. (B) A comparison of eATP hydrolysis using 12 μM of either [α-^{32}P]ATP or [γ-^{32}P]ATP. Results were expressed as percentage of the total ATP hydrolyzed at each time point and were calculated from data obtained in Figs. 8A and 9A. The continuous lines represent fittings of exponential functions to experimental data.

[eATP] remain stable. Addition of hypotonic medium (180 mOsm) to cultured cells triggered ATP release (Fig. 10A), with resulted in an approximately 70% increase in [eATP] (from 115 ± 2.1 nM to 198 ± 2.8 nM). A mechanical perturbation was created by stimulating cells with isotonic medium, causing an increase [eATP] of approx. 30% (from 131 ± 2.9 nM to 170 ± 3.2 nM) (Fig. 10A).

To rule out the possibility that cell lysis due to hypotonic shock could contribute to the increase in [eATP], we assessed cell viability 30 min after cells were exposed to iso- and hypotonic conditions. Viability was similar before and after addition of each stimulus (Fig. 10B), indicating that no lytic release of ATP was induced.

Since hypotonicity affected ATP release, we wondered whether this stimulus could also affect ectoATPase activity. Thus appV$_{max}$ were estimated from the time course of [^{32}P]Pi accumulation released using 500 μM concentration of [γ-^{32}P]ATP under iso- and hypotonic conditions. As seen in Fig. S1A, similar values of appVmax were obtained under both conditions (11.35 ± 0.9 pmol [^{32}P]Pi/μg protein/min in isotonic medium vs 11.07 ± pmol [^{32}P]Pi/μg of protein/min in hypotonic medium). Moreover, using the malachite green method, we also observed that, in hypotonic media without Pi, rates of ectoATPase (Fig. S1B), ectoADPase (Fig. S1C) and ectoAMPase (Fig. S1D) activities

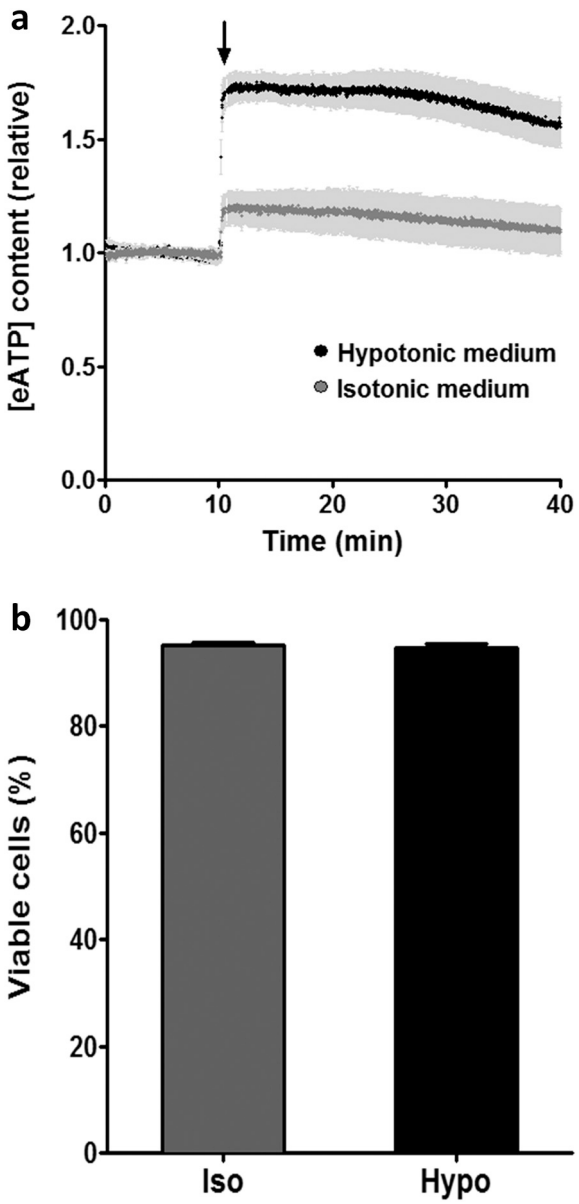

Fig. 10. eATP kinetics of hypotonically- and mechanically-stimulated Caco-2 cells.
The time course of [eATP] from Caco-2 cells was quantified by real-time luminometry performed at room temperature. (A) Cells were maintained in isotonic medium and, at the times indicated by the arrow, were exposed to isotonic medium (grey, $N = 5$ independent experiments run in triplicate) or to 180 mOsm hypotonic medium (black, N = 8). Levels of eATP were normalized to the baseline before the addition of hypo- or isotonic media and are expressed as means of relative [eATP] ± s.e.m. (B) Viability of Caco-2 cells was measured by Trypan Blue exclusion. Cells were exposed to isotonic (grey) or hypotonic (black) media for 30 min. Results represent means ± s.e.m. (N = 4 independent experiments run in triplicate) and are expressed as percentages of total cells. (For interpretation of the references to color in this figure legend, the reader is referred to the web version of this article.)

were similar to those found in isotonic media. Finally, as observed for ectonucleotidase activities, ectophosphatase activity (i.e., pNPP hydrolysis) was not modified by the hypotonic treatment (Fig. S1E).

3.7. Predictions of eATP kinetics

As mentioned above, a data-driven algorithm was run to analyze the contribution of ATP efflux and ectoATPase activity to eATP kinetics of Caco-2 cells, where eATP concentration should increase by ATP efflux, and decrease by eATP hydrolysis. Such analysis is possible since the ectoATPase substrate curve (Fig. 8) can be used to calculate the contribution of eATP hydrolysis to eATP concentration along the eATP kinetics curve. In this way, ATP efflux can be derived from the eATP kinetics curve.

Accordingly, Fig. 11 shows the experimental eATP kinetics (black symbol), the predicted kinetics of eATP consumption by ectoATPase activity (red symbol), and the prediction of eATP kinetics under a condition where the effect of ectoATPase activity was subtracted (blue symbol). Predictions were made for experiments using hypotonic (Fig. 11A) and mechanical (Fig. 11B) stimuli. Interestingly, blockage of eATP hydrolysis only slightly changed the acute phase of [eATP] increase at 40 s post-stimulus. However, at later times, ectoATPase activity fully counterbalanced the relatively low constitutive ATP release. The transient nature of post stimulus ATP efflux, which activates and deactivates in about 10 s, is illustrated in Fig. 11C. It can be seen that stimuli triggered a three orders of magnitude increase of ATP efflux, which peaked at 3486 nM/min (hypotonic stimulus) and 1785 nM/min (mechanical stimulus) after the treatments.

4. Discussion

Intestinal epithelial cells are able to release nucleotides and exhibit several ectonucleotidases capable of controlling the rate, amount and metabolism of nucleotides at the cell surface. In this context, the main goal of this study was to identify and characterize functional ectonucleotidases in Caco-2 cells, a cell model of epithelial enterocytes [45]. Kinetic experiments were performed using intact viable cells, thus assessing the capacity of Caco-2 cells to mediate hydrolysis of ATP and by-products at the cell surface by different ectoenzymes. In addition, to get an integrative insight into eATP regulation of Caco-2 cells, we analyzed how eATP hydrolysis and intracellular ATP release contribute to the kinetics of eATP accumulation (i.e., eATP kinetics).

4.1. NTPDases and 5′NT

Studies using intact viable Caco-2 cells exposed to AMP, ADP and ATP showed high ATPase activity, intermediate AMPase activity, and relatively low ADPase activity (Fig. 1). These results are consistent with the presence of one or more NTPDases, and 5′NT [23]. Accordingly, western blot combined with immunolocalization analysis allowed us to identify NTPDase1, -2 and 5′NT expressed on the cell membrane of Caco-2 cells, while NTPDases3 and -8 were not detected (Figs. 2 and 3). Experiments performed in a mouse model showed that NTPDase3 is present in neurons of the myenteric and submucosal plexus, but not in epithelial cells [46], in agreement with this study. On the other hand, the human colorectal adenocarcinoma HT29 cells expressed functional NTPDase 2 and 5′NT, but no NTPDase1, while neither NTPDase 3 nor NTPDase 8 were not detected [47].

In addition to studying the nucleotide kinetic profile and cell membrane immunolocalization of NTPDases, we tested the effects of POM-1, an inhibitor of NTPDases [41,48], which proved effective in inhibiting ATP hydrolysis, while its inhibitory effect on AMP hydrolysis, as expected, was lower (Fig. 1C) [49,50] .

4.2. NPPases and ectophosphatases

In looking for other enzymes acting as eATP consumers, we checked the potential contribution of ectophosphodiesterase and/or ectophosphatase activities. Members of the NPPase family were described in differentiated Caco-2 cells [51] and mice small intestinal epithelia [52]. Assuming that Caco-2 cells would activate ATP to AMP conversion by one or more NPPs, thereby contributing to eATP consumption, then PPi should accumulate in the assay medium. However, no PPi production was detected (Fig. 4), thus discarding the presence of functional

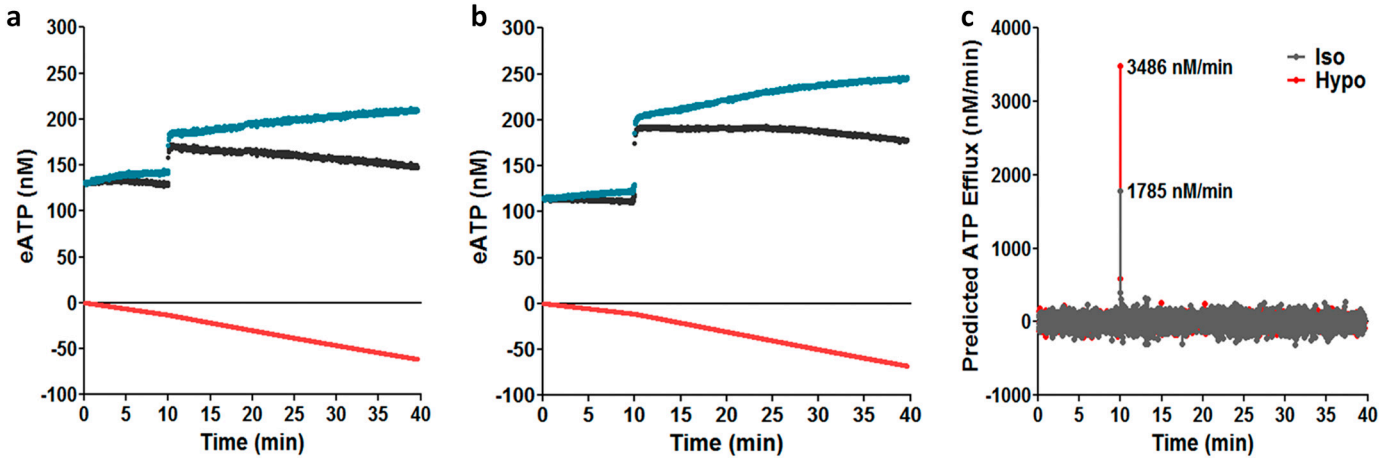

Fig. 11. Predictions of eATP kinetics. Theoretical curves showing the effect of eATP hydrolysis and ATP release on eATP kinetics. (A, B) The linear equation describing ectoATPase activity vs [ATP] used in Fig. 8 was used to calculate eATP consumption at every time point of the eATP kinetics curve of Fig. 9. Then, the values of eATP consumption obtained were used to calculate the accumulated [eATP] consumed during eATP kinetics, thus generating the ectoATPase curve (red symbols). By subtracting the contribution of this ectoATPase curve to the experimental eATP kinetics (black symbols), a predicted eATP kinetics (blue symbols) was calculated where the effects of ectoATPase activity were mathematically eliminated. The results are expressed as nM/well for mechanical (A) and hypotonic stimuli (B). (C) The predicted eATP efflux (nM/min) was calculated by numerical differentiation of the predicted eATP kinetics obtained in B. (For interpretation of the references to color in this figure legend, the reader is referred to the web version of this article.)

NPPases.

Regarding the role of ectophosphatases, early studies showed ALP purified from intestinal mucosa to exhibit an alkaline pH optimum [53], while purified ALPs from liver and intestine displayed maximal activities at neutral pH [54,55]. Using media at near neutral pH we showed that Caco-2 cells exhibited significant pNPP hydrolysis, which according to complementary pH curves represents the optimal pH for ectophosphatase activity (Fig. 5).

Molybdate, a phosphatases inhibitor [44], highly reduced both appV_{max} and pNPP app. affinity (Fig. 5A), but did not affect eATP hydrolysis (Fig. 7A), whereas POM-1, a competitive inhibitor of ALP [49,56], reduced app. Affinity but left appV_{max} unaltered (Fig. 5C).

Various reports show that ALPs exhibit wide substrate specificity towards nucleotides and other substrates [23]. Interestingly in this context, exposure of Caco-2 cells to ATP, ADP or AMP was able to inhibit pNPP hydrolysis in a concentration dependent manner, with AMP showing the strongest effect, followed by ADP and ATP (Fig. 6).

Ectophosphatase of Caco-2 cells was strongly inhibited by medium Pi. In humans, the Pi concentration in the intestinal lumen is variable (0.75–17.5 mM), depending on the dietary Pi load [57], while serum Pi is usually maintained between 0.75 and 1.45 mM [58]. Thus the contribution of ectophosphatase activity to eATP hydrolysis in Caco-2 cells may vary, showing activation as Pi content is reduced (Fig. 7B). On the contrary, NTPDases were not affected by Pi, and should therefore show unaltered activity in the face of a Pi changing environment.

4.3. eATP regulation at low micromolar ATP

To gain insight into the physiological role of eATP, the rates of eATP hydrolysis and intracellular ATP release were studied. Firstly, eATP hydrolysis was tested using [γ^{32}P]ATP and ATP concentrations in the low micromolar range, within the range of affinities for most P2X (except P2X7) and P2Y receptors [17]. Results showed a significant rate of ectoATPase activity of intact cells, which increased linearly with [eATP]. The linearity of the substrate curve was expected, considering that ATP concentrations used lay well below the reported values of Km_{ATP} for ectonucleotidases in several cell systems [24,59,60].

Another kinetic parameter refers to the K_{ATP}, i.e., the slope of the substrate curve. Table 1 depicts values of K_{ATP} of this study and those of other cell systems and organisms. All these K_{ATP} values originate from measurements made under similar conditions and carried out using intact cells and low micromolar eATP concentrations. The graph shows that Caco-2 cells display an intermediate value of K_{ATP}; it was similar to that found in renal cortical collecting duct cells [61], much higher than those found in human RBCs and bacteria [62–64], but significantly lower than K_{ATP} values of hepatic cells [30].

To better understand the role of ectoATPase activity of Caco-2 cells, we use online luminometry to assess eATP kinetics, which depends on ATP release and eATP hydrolysis. ATP and other nucleotides are released into the extracellular medium under physio- and pathological conditions [65–68]. In particular, hypotonic stress constitutes a proinflammatory signal in Caco-2 cells, and has been shown to induce ATP release in intestinal cell and other cell types [69–74]. Our experiments showed that mechanical stress, as well as hypotonicity, caused accumulation of endogenous eATP, which implies activation of ATP exit mechanisms.

Table 1
Values of K_{ATP} estimated from different cells types.
Results represent the slope of curves describing EctoATPase activity vs [ATP] for Caco-2 cells (this study), and several other cells types. All values were obtained by incubating intact cells in the presence of different concentrations of [γ-^{32}P]-ATP in the low micromolar range.

Cellular type	K_{ATP} (pmol/10^6 cells/min/nM)	Reference
Escherichia coli	3.7×10^{-07}	Alvarez et al., 2017 [63]
Human red blood cells	1.16×10^{-5}	Montalbetti et al., 2011 [62] Leal Denis et al., 2019 [64]
Human colorectal adenocarcinoma Caco-2 cells	1.5×10^{-2}	This study
Differentiated human colorectal adenocarcinoma Caco-2 cells (apical domain)	1.8×10^{-2}	Alvarez et al., 2017 [63]
Rat renal cortical collecting ducts cells (RCCD)	2×10^{-2}	Pizzoni et al., 2021 [61]
Rainbow trout *Oncorhynchus mykiss* hepatocytes	6×10^{-2}	Pafundo et al., 2004 [81]
Goldfish *Carassius auratus* hepatocytes	0.10	Pafundo et al., 2008 [39]
Human hepatoma cells Huh-7 cells	0.17	Espelt et al., 2013 [30]

Caco-2 cells produced ATP mostly by oxidative metabolism [75], and displayed a steady intracellular ATP concentration of approx. 20 ng/μg protein [76]. Considering this figure, the observed [eATP] increase following mechanical and hypotonic stimuli is expected to require only 0.3–0.5% of the available intracellular ATP, i.e., ATP efflux does not impose an energetic burden to the cells.

Regarding the factors affecting eATP kinetics, any observed [eATP] increase should be counteracted by ectoATPase activity, which as mentioned above, must increase linearly with [eATP]. Running a data-driven algorithm allowed us to quantify the contribution of ATP release and eATP hydrolysis to eATP kinetics. Results showed ATP efflux to be small under unstimulated conditions. However, following stimulation, ATP efflux showed a steep 1800–3500 fold increase in less than 1 min, followed by an equally rapid decay to basal levels (Fig. 11). The observed strong ATP efflux is compatible with activation of conductive channels and pores on the cell membrane. Since [eATP] is much lower than intracellular [ATP], such ATP efflux may be driven by the steep electrochemical (mostly chemical) gradient across the plasma membrane, as observed in other cell types [61,62,77]. As shown in Fig. 11, within the first min post stimulus phase, the contribution of eATP hydrolysis to eATP kinetics was negligible. However, for the rest of the incubation period, ATP efflux strongly decreased, thereby allowing ectoATPase activity to control eATP kinetics. Overall, this analysis shows that mechanical and hypotonic perturbation of Caco-2 cells can lead to strong but brief eATP release, which is sufficiently high to activate most ATP-P receptors on the cell surface, followed by inactivation of the purinergic response by ectoATPase activity.

4.4. Sequential dephosphorylation of ATP

Having detected 5′-NT by facilitated AMP hydrolysis, western blot and immunofluorescence analysis, we wondered whether 5′-NT may act in concert with NTPDases at relatively low substrate concentrations, as demonstrated in other cell systems [8,23]. To this end, we exposed Caco-2 cells to a low μM [α^{32}P]ATP concentration. In the absence of NPPase activity, [α^{32}P]Pi release may be expected only if ectonucleotidases were present that sequentially liberate γ-, β- and α-Pi of ATP at the cell surface, thus producing one ADO for every [α^{32}P]Pi produced. Accordingly, addition of [α^{32}P]ATP led to [α^{32}P]Pi release, thus providing the first evidence that eATP is fully dephosphorylated in Caco-2 cells. Release of [α^{32}P]Pi was significantly lower than that of [γ^{32}P]Pi. This lower rate of the former was expected, since under eATP exposure the effective extracellular AMP concentration sensed by 5′NT is limited by the velocities of ATP and ADP hydrolysis. Nevertheless ectoAMPase activity was significant, and is in line with $K_{0.5}$ values of 5′NTs found in the low micromolar range [23].

The observed production of ATP-derived ADO may activate one or more subtypes of P1 receptors present in Caco-2 cells [78]. A number of studies have implicated adenosine P1 receptors in limiting inflammation in the gastrointestinal system [79], counteracting the pro-inflammatory actions of eATP on P2X7 receptor [19]. Moreover, in the colonic epithelium P1 receptors play an important role in regulating water and Cl^- secretion [80]. In Caco-2 and HCT8 intestinal cell lines, the concerted action of eATP, acting on P2 receptors, and adenosine, acting on P1 receptors, was shown to regulate proliferation and apoptosis [28], while Cl^- secretion of Caco-2 cells was regulated by eATP and other extracellular nucleotides, suggesting the participation of P2Y receptors in the response [10].

5. Conclusions

We have characterized the capacity of Caco-2 cells to hydrolyze extracellular ATP, ADP and AMP, and identified NTPDase1 and 2, 5′NT and a neutral ectophosphatase as the main ectonucleotidases in these cells. Ectophosphatase, unlike NTPDases, was affected by the available Pi content of the extracellular milieu. The catalytic properties of ectoATPase activity were unaffected by hypotonicity. Cytosolic ATP was released acutely following physiological stimuli, with almost no energy cost. The accumulated eATP was subsequently hydrolyzed by ectoATPase activity, thus shaping the late phase of eATP kinetics. Caco-2 cells were able to sequentially dephosphorylate ATP to adenosine, thus allowing sequential P2 and P1 receptor signaling.

Future studies would allow elucidating the modulation of nucleotide-dependent cellular responses in the epithelial barrier of the intestine, such as inflammation, proliferation, apoptosis, electrolytes transport and cell volume regulation.

Supplementary data to this article can be found online at https://doi.org/10.1016/j.bbamem.2021.183679.

Declaration of competing interest

The authors declare that they have no known competing financial interests or personal relationships that could have appeared to influence the work reported in this paper.

Acknowledgments

We are grateful to Dr. Julie Pelletier for her helpful technical advice regarding the use of antibodies anti-ectonucleotidases for western blot.

This work was supported by CONICET (Grant PIP 112 201501 00459); the Universidad de Buenos Aires (Grant 200201701001 52BA, PDE 45 2020); the Agencia Nacional de Promoción Científica y Técnica (PICT 00905, ECOS Sud A15S01); the Laboratory of Excellence GR-Ex (Grant ANR-11-LABX-0051). Julieta Schachter, C.L.A., MPF, GC, RG-Land P.J.S. are career researchers at Consejo Nacional de Investigaciones Científicas y Técnicas (CONICET). ZB is a doctoral student and MPM is a postdoctoral fellow from CONICET.

Jean Sévigny received support from the Canadian Institutes of Health Research (PJT - 156205).

MAO was funded by grants from the French National Research Agency (ANR-11-LABX-005).

The funders had no role in study design, data collection and analysis, decision to publish, or preparation of the manuscript.

References

[1] N. Mikolajewicz, A. Mohammed, M. Morris, S.V. Komarova, Meta-analysis of mechanically-stimulated ATP release from mammalian cells, J. Cell Sci. (2018), https://doi.org/10.1242/jcs.223354.

[2] M. Verónica Donoso, F. Hernández, T. Villalón, C. Acuña-Castillo, J. Pablo Huidobro-Toro, Pharmacological dissection of the cellular mechanisms associated to the spontaneous and the mechanically stimulated ATP release by mesentery endothelial cells: roles of thrombin and TRPV, Purinergic Signalling 14 (2018) 121–139, https://doi.org/10.1007/s11302-017-9599-7.

[3] M. Sridharan, S.P. Adderley, E.A. Bowles, T.M. Egan, A.H. Stephenson, M. L. Ellsworth, et al., Pannexin 1 is the conduit for low oxygen tension-induced ATP release from human erythrocytes, Am. J. Phys. Heart Circ. Phys. 299 (2010) H1146–H1152, https://doi.org/10.1152/ajpheart.00301.2010.

[4] J.K. Crane, T.M. Naeher, S.S. Choudhari, E.M. Giroux, Two pathways for ATP release from host cells in enteropathogenic Escherichia coli infection, Am. J. Physiol. Gastrointest. Liver Physiol. 289 (2005) G407–G417, https://doi.org/10.1152/ajpgi.00137.2005.

[5] A. Piccini, S. Carta, S. Tassi, D. Lasiglie, G. Fossati, A. Rubartelli, ATP is released by monocytes stimulated with pathogen-sensing receptor ligands and induces IL-1 and IL-18 secretion in an autocrine way, Proc. Natl. Acad. Sci. 105 (2008) 8067–8072, https://doi.org/10.1073/pnas.0709684105.

[6] Y. Wang, R. Roman, S.D. Lidofsky, J.G. Fitz, Autocrine signaling through ATP release represents a novel mechanism for cell volume regulation, Proc. Natl. Acad. Sci. 93 (1996) 12020–12025, https://doi.org/10.1073/pnas.93.21.12020.

[7] S. Tatur, S. Kreda, E. Lazarowski, R. Grygorczyk, Calcium-dependent release of adenosine and uridine nucleotides from A549 cells, Purinergic Signalling 4 (2008) 139–146, https://doi.org/10.1007/s11302-007-9059-x.

[8] D.E. Pafundo, C.L. Alvarez, G. Krumschnabel, P.J. Schwarzbaum, A volume regulatory response can be triggered by nucleosides in human erythrocytes, a perfect osmometer no longer, J. Biol. Chem. 285 (2010) 6134–6144, https://doi.org/10.1074/jbc.M109.078246.

[9] L.Y. Korman, G.F. Lemp, M.J. Jackson, J.D. Gardner, Mechanism of action of ATP on intestinal epithelial cells, Biochim. Biophys. Acta, Mol. Cell Res. 721 (1982) 47–54, https://doi.org/10.1016/0167-4889(82)90022-2.

[10] C.N. Inoue, J.S. Woo, E.M. Schwiebert, T. Morita, K. Hanaoka, S.E. Guggino, et al., Role of purinergic receptors in chloride secretion in Caco-2 cells, Am. J. Phys. Cell Phys. 272 (1997) C1862–C1870, https://doi.org/10.1152/ajpcell.1997.272.6.C1862.
[11] T. Yamamoto, Y. Suzuki, Role of luminal ATP in regulating electrogenic Na+ absorption in Guinea pig distal colon, Am. J. Physiol. Gastrointest. Liver Physiol. 283 (2002) G300–G308, https://doi.org/10.1152/ajpgi.00541.2001.
[12] X. Dong, E.J. Smoll, K.H. Ko, J. Lee, J.Y. Chow, H.D. Kim, et al., P2Y receptors mediate ca 2+ signaling in duodenocytes and contribute to duodenal mucosal bicarbonate secretion, Am. J. Physiol. Gastrointest. Liver Physiol. 296 (2009) G424–G432, https://doi.org/10.1152/ajpgi.90314.2008.
[13] G. Arguin, J.-F. Bourzac, M. Placet, C.M. Molle, M. Paquette, J.-F. Beaudoin, et al., The loss of P2X7 receptor expression leads to increase intestinal glucose transit and hepatic steatosis, Sci. Rep. 7 (2017) 12917, https://doi.org/10.1038/s41598-017-13300-8.
[14] G. Burnstock, Purinergic signalling in the gastrointestinal tract and related organs in health and disease, Purinergic Signalling. 10 (2014) 3–50, https://doi.org/10.1007/s11302-013-9397-9.
[15] I. von Kügelgen, K. Hoffmann, Pharmacology and structure of P2Y receptors, Neuropharmacology 104 (2016) 50–61, https://doi.org/10.1016/j.neuropharm.2015.10.030.
[16] A.A. Welihinda, M. Kaur, K. Greene, Y. Zhai, E.P. Amento, The adenosine metabolite inosine is a functional agonist of the adenosine A2A receptor with a unique signaling bias, Cell. Signal. 28 (2016) 552–560, https://doi.org/10.1016/j.cellsig.2016.02.010.
[17] G. Burnstock, Purine and purinergic receptors, Brain Neurosci. Adv. 2 (2018), 239821281881749, https://doi.org/10.1177/2398212818817494.
[18] R. Corriden, P.A. Insel, Basal release of ATP: an autocrine-paracrine mechanism for cell regulation, Sci. Signal. 3 (2010), re1-re1, https://doi.org/10.1126/scisignal.3104re1.
[19] C.O. Souza, G.F. Santoro, V.R. Figliuolo, H.F. Nanini, H.S.P. de Souza, M.T. L. Castelo-Branco, et al., Extracellular ATP induces cell death in human intestinal epithelial cells, Biochim. Biophys. Acta Gen. Subj. 1820 (2012) 1867–1878, https://doi.org/10.1016/j.bbagen.2012.08.013.
[20] Y. Kurashima, T. Amiya, T. Nochi, K. Fujisawa, T. Haraguchi, H. Iba, et al., Extracellular ATP mediates mast cell-dependent intestinal inflammation through P2X7 purinoceptors, Nat. Commun. 3 (2012) 1034, https://doi.org/10.1038/ncomms2023.
[21] A. Cesaro, P. Brest, V. Hofman, X. Hébuterne, S. Wildman, B. Ferrua, et al., Amplification loop of the inflammatory process is induced by P2X 7 R activation in intestinal epithelial cells in response to neutrophil transepithelial migration, Am. J. Physiol. Gastrointest. Liver Physiol. 299 (2010) G32–G42, https://doi.org/10.1152/ajpgi.00282.2009.
[22] G.G. Yegutkin, Nucleotide- and nucleoside-converting ectoenzymes: Important modulators of purinergic signalling cascade, Biochim. Biophys. Acta Mol. Cell Res. 1783 (2008) 673–694, https://doi.org/10.1016/j.bbamcr.2008.01.024.
[23] H. Zimmermann, History of ectonucleotidases and their role in purinergic signaling, Biochem. Pharmacol. 187 (2021), 114322, https://doi.org/10.1016/j.bcp.2020.114322.
[24] F. Kukulski, S.A. Lévesque, É.G. Lavoie, J. Lecka, F. Bigonnesse, A.F. Knowles, et al., Comparative hydrolysis of P2 receptor agonists by NTPDases 1, 2, 3 and 8, Purinergic Signalling. 1 (2005) 193–204, https://doi.org/10.1007/s11302-005-6217-x.
[25] S.C. Robson, J. Sévigny, H. Zimmermann, The E-NTPDase family of ectonucleotidases: structure function relationships and pathophysiological significance, Purinergic Signalling. 2 (2006) 409–430, https://doi.org/10.1007/s11302-006-9003-5.
[26] J.W. Goding, B. Grobben, H. Slegers, Physiological and pathophysiological functions of the ecto-nucleotide pyrophosphatase/phosphodiesterase family, Biochim. Biophys. Acta, Mol. Basis Dis. 1638 (2003) 1–19, https://doi.org/10.1016/S0925-4439(03)00058-9.
[27] J. Bilski, A. Mazur-Bialy, D. Wojcik, J. Zahradnik-Bilska, B. Brzozowski, M. Magierowski, et al., The role of intestinal alkaline phosphatase in inflammatory disorders of gastrointestinal tract, Mediat. Inflamm. 2017 (2017) 1–9, https://doi.org/10.1155/2017/9074601.
[28] R. Coutinho-Silva, L. Stahl, K.-K. Cheung, N.E. de Campos, C. de Oliveira Souza, D. M. Ojcius, P2X and P2Y purinergic receptors on human intestinal epithelial carcinoma cells: effects of extracellular nucleotides on apoptosis and cell proliferation, Am. J. Physiol. Gastrointest. Liver Physiol. 288 (2005), G1024–G1035, https://doi.org/10.1152/ajpgi.00211.2004.
[29] P.A. Lanzetta, L.J. Alvarez, P.S. Reinach, O.A. Candia, An improved assay for nanomole amounts of inorganic phosphate, Anal. Biochem. 100 (1979) 95–97, https://doi.org/10.1016/0003-2697(79)90115-5.
[30] M.V. Espelt, F. de Tezanos Pinto, C.L. Alvarez, G.S. Alberti, J. Incicco, M.F.L. Denis, et al., On the role of ATP release, ectoATPase activity, and extracellular ADP in the regulatory volume decrease of Huh-7 human hepatoma cells, Am. J. Physiol. Cell 304 (2013) C1013–C1026, https://doi.org/10.1152/ajpcell.00254.2012.
[31] J. Sévigny, E. Kaczmarek, J.B. Siegel, M. Imai, K. Koziak, J. Schulte am Esch, Structural elements and limited proteolysis of CD39 influence ATP diphosphohydrolase activity†, Biochemistry 38 (1999) 2248–2258, https://doi.org/10.1021/bi982426k.
[32] J. Pelletier, H. Agonsanou, N. Delvalle, M. Fausther, M. Salem, B. Gulbransen, et al., Generation and characterization of polyclonal and monoclonal antibodies to human NTPDase2 including a blocking antibody, Purinergic Signalling. 13 (2017) 293–304, https://doi.org/10.1007/s11302-017-9561-8.
[33] M.N. Munkonda, J. Pelletier, V.V. Ivanenkov, M. Fausther, A. Tremblay, B. Künzli, et al., Characterization of a monoclonal antibody as the first specific inhibitor of human NTP diphosphohydrolase-3, FEBS J. 276 (2009) 479–496, https://doi.org/10.1111/j.1742-4658.2008.06797.x.
[34] J. Pelletier, M. Salem, J. Lecka, M. Fausther, F. Bigonnesse, J. Sévigny, Generation and Characterization of Specific Antibodies to the Murine and Human Ectonucleotidase NTPDase8, 2017, https://doi.org/10.3389/fphar.2017.00115.
[35] L.R. Mazzitelli, H.P. Adamo, The phosphatase activity of the plasma membrane Ca2 + pump. Activation by acidic lipids in the absence of Ca2+ increases the apparent affinity for Mg2, Biochim. Biophys. Acta Biomembr. 1768 (2007) 1777–1783, https://doi.org/10.1016/j.bbamem.2007.04.019.
[36] M. Bradford, A rapid and sensitive method for the quantitation of microgram quantities of protein utilizing the principle of protein-dye binding, Anal. Biochem. 72 (1976) 248–254, https://doi.org/10.1006/abio.1976.9999.
[37] U.K. Laemmli, Cleavage of structural proteins during the assembly of the head of bacteriophage T4, Nature 227 (1970) 680–685, https://doi.org/10.1038/227680a0.
[38] B.L. Strehler, in: Bioluminescence Assay: Principles and Practice, 2006, pp. 99–181, https://doi.org/10.1002/9780470110348.ch2.
[39] D.E. Pafundo, O. Chara, M.P. Faillace, G. Krumschnabel, P.J. Schwarzbaum, Kinetics of ATP release and cell volume regulation of hyposmotically challenged goldfish hepatocytes, Am. J. Phys. Regul. Integr. Comp. Phys. 294 (2008) R220–R233, https://doi.org/10.1152/ajpregu.00522.2007.
[40] M.W. Gorman, D.R. Marble, K. Ogimoto, E.O. Feigl, Measurement of adenine nucleotides in plasma, Luminescence 18 (2003) 173–181, https://doi.org/10.1002/bio.721.
[41] C.E. Müller, J. Iqbal, Y. Baqi, H. Zimmermann, A. Röllich, H. Stephan, Polyoxometalates—a new class of potent ecto-nucleoside triphosphate diphosphohydrolase (NTPDase) inhibitors, Bioorg. Med. Chem. Lett. 16 (2006) 5943–5947, https://doi.org/10.1016/j.bmcl.2006.09.003.
[42] S. Baltes, H. Nau, A. Lampen, All-trans retinoic acid enhances differentiation and influences permeability of intestinal Caco-2 cells under serum-free conditions, Develop. Growth Differ. 46 (2004) 503–514, https://doi.org/10.1111/j.1440-169x.2004.00765.x.
[43] M. Mizumori, M. Ham, P.H. Guth, E. Engel, J.D. Kaunitz, Y. Akiba, Intestinal alkaline phosphatase regulates protective surface microclimate pH in rat duodenum, J. Physiol. 587 (2009) 3651–3663, https://doi.org/10.1113/jphysiol.2009.172270.
[44] Y. Lindqvist, G. Schneider, P. Vihko, Crystal structures of rat acid phosphatase complexed with the transition-state analogs vanadate and molybdate. Implications for the reaction mechanism, Eur. J. Biochem. 221 (1994) 139–142, https://doi.org/10.1111/j.1432-1033.1994.tb18722.x.
[45] I.J. Hidalgo, T.J. Raub, R.T. Borchardt, Characterization of the human colon carcinoma cell line (Caco-2) as a model system for intestinal epithelial permeability, Gastroenterology 96 (1989) 736–749, https://doi.org/10.1016/S0016-5085(89)80072-1.
[46] E.G. Lavoie, B.D. Gulbransen, M. Martín-Satué, E. Aliagas, K.A. Sharkey, J. Sévigny, Ectonucleotidases in the digestive system: focus on NTPDase3 localization, Am. J. Physiol. Gastrointest. Liver Physiol. 300 (2011), G608-G620, https://doi.org/10.1152/ajpgi.00207.2010.
[47] F. Bahrami, F. Kukulski, J. Lecka, A. Tremblay, J. Pelletier, L. Rockenbach, et al., Purine-metabolizing ectoenzymes control IL-8 production in human colon HT-29 cells, Mediat. Inflamm. 2014 (2014) 1–10, https://doi.org/10.1155/2014/879895.
[48] M.J. Wall, G. Wigmore, J. Lopatár, B.G. Frenguelli, N. Dale, The novel NTPDase inhibitor sodium polyoxotungstate (POM-1) inhibits ATP breakdown but also blocks central synaptic transmission, an action independent of NTPDase inhibition, Neuropharmacology 55 (2008) 1251–1258, https://doi.org/10.1016/j.neuropharm.2008.08.005.
[49] S.-Y. Lee, A. Fiene, W. Li, T. Hanck, K.A. Brylev, V.E. Fedorov, et al., Polyoxometalates—potent and selective ecto-nucleotidase inhibitors, Biochem. Pharmacol. 93 (2015) 171–181, https://doi.org/10.1016/j.bcp.2014.11.002.
[50] S.A. Goueli, K. Hsiao, Monitoring and characterizing soluble and membrane-bound ectonucleotidases CD73 and CD39, PLoS One. 14 (2019), e0220094, https://doi.org/10.1371/journal.pone.0220094.
[51] N.R. Meerson, V. Bello, J.L. Delaunay, T.A. Slimane, D. Delautier, C. Lenoir, et al., Intracellular traffic of the ecto-nucleotide pyrophosphatase/phosphodiesterase NPP3 to the apical plasma membrane of MDCK and Caco-2 cells: apical targeting occurs in the absence of N-glycosylation, J. Cell Sci. 113 (2000) 4193–4202, https://doi.org/10.1242/jcs.113.23.4193.
[52] Y. Furuta, S.-H. Tsai, M. Kinoshita, K. Fujimoto, R. Okumura, E. Umemoto, et al., E-NPP3 controls plasmacytoid dendritic cell numbers in the small intestine, PLoS One. 12 (2017), e0172509, https://doi.org/10.1371/journal.pone.0172509.
[53] H. Fernley, P. Walker, Studies on alkaline phosphatase. Inhibition by phosphate derivatives and the substrate specificity, Biochem. J. 104 (1967) 1011–1018, https://doi.org/10.1042/bj1041011.
[54] J.R. Chan, R.A. Stinson, Dephosphorylation of phosphoproteins of human liver plasma membranes by endogenous and purified liver alkaline phosphatases, J. Biol. Chem. 261 (1986) 7635–7639. http://www.ncbi.nlm.nih.gov/pubmed/3011792.
[55] G. Swarup, S. Cohen, D.L. Garbers, Selective dephosphorylation of proteins containing phosphotyrosine by alkaline phosphatases, J. Biol. Chem. 256 (1981) 8197–8201. http://www.ncbi.nlm.nih.gov/pubmed/6167574.
[56] R. Raza, A. Matin, S. Sarwar, M. Barsukova-Stuckart, M. Ibrahim, U. Kortz, et al., Polyoxometalates as potent and selective inhibitors of alkaline phosphatases with profound anticancer and amoebicidal activities, Dalton Trans. 41 (2012) 14329, https://doi.org/10.1039/c2dt31784b.

[57] G.R. Davis, J.E. Zerwekh, T.F. Parker, G.J. Krejs, C.Y. Pak, J.S. Fordtran, Absorption of phosphate in the jejunum of patients with chronic renal failure before and after correction of vitamin D deficiency, Gastroenterology 85 (1983) 908–916. http://www.ncbi.nlm.nih.gov/pubmed/6688402.
[58] S. Jeffrey, E. Lerma, A.N. Berns A, Current Diagnosis and Treatment: Nephrology and Hypertension, McGraw-Hil, London, 2018.
[59] S.L. Henz, C.G. Ribeiro, A. Rosa, R.A. Chiarelli, E.A. Casali, J.J.F. Sarkis, Kinetic characterization of ATP diphosphohydrolase and 5'-nucleotidase activities in cells cultured from submandibular salivary glands of rats, Cell Biol. Int. 30 (2006) 214–220, https://doi.org/10.1016/j.cellbi.2005.10.027.
[60] A. Buffon, V.B. Ribeiro, M.R. Wink, E.A. Casali, J.J.F. Sarkis, Nucleotide metabolizing ecto-enzymes in Walker 256 tumor cells: molecular identification, kinetic characterization and biochemical properties, Life Sci. 80 (2007) 950–958, https://doi.org/10.1016/j.lfs.2006.11.024.
[61] A. Pizzoni, Z. Bazzi, G. Di Giusto, C.L. Alvarez, V. Rivarola, C. Capurro, et al., Release of ATP by TRPV4 activation is dependent upon the expression of AQP2 in renal cells, J. Cell. Physiol. 236 (2021) 2559–2571, https://doi.org/10.1002/jcp.30013.
[62] N. Montalbetti, M.F. Leal Denis, O.P. Pignataro, E. Kobatake, E.R. Lazarowski, P. J. Schwarzbaum, Homeostasis of extracellular ATP in human erythrocytes*, J. Biol. Chem. 286 (2011) 38397–38407, https://doi.org/10.1074/jbc.M111.221713.
[63] C.L. Alvarez, G. Corradi, N. Lauri, I. Marginedas-Freixa, M.F. Leal Denis, N. Enrique, et al., Dynamic regulation of extracellular ATP in Escherichia coli, Biochem. J. 474 (2017) 1395–1416, https://doi.org/10.1042/BCJ20160879.
[64] M.F. Leal Denis, S.D. Lefevre, C.L. Alvarez, N. Lauri, N. Enrique, D.E. Rinaldi, et al., Regulation of extracellular ATP of human erythrocytes treated with a-hemolysin. Effects of cell volume, morphology, rheology and hemolysis, Biochim. Biophys. Acta Mol. Cell Res. 1866 (2019) 896–915, https://doi.org/10.1016/j.bbamcr.2019.01.018.
[65] A.K. Dutta, R.Z. Sabirov, H. Uramoto, Y. Okada, Role of ATP-conductive anion channel in ATP release from neonatal rat cardiomyocytes in ischaemic or hypoxic conditions, J. Physiol. 559 (2004) 799–812, https://doi.org/10.1113/jphysiol.2004.069245.
[66] A.P. Feranchak, M.A. Lewis, C. Kresge, M. Sathe, A. Bugde, K. Luby-Phelps, et al., Initiation of purinergic signaling by exocytosis of ATP-containing vesicles in liver epithelium, J. Biol. Chem. 285 (2010) 8138–8147, https://doi.org/10.1074/jbc.M109.065482.
[67] J.G. Fitz, Regulation of cellular ATP release, Trans. Am. Clin. Climatol. Assoc. 118 (2007) 199–208. http://www.ncbi.nlm.nih.gov/pubmed/18528503.
[68] E.R. Lazarowski, Vesicular and conductive mechanisms of nucleotide release, Purinergic Signalling. 8 (2012) 359–373, https://doi.org/10.1007/s11302-012-9304-9.
[69] T. Koyama, M. Oike, Y. Ito, Involvement of Rho-kinase and tyrosine kinase in hypotonic stress-induced ATP release in bovine aortic endothelial cells, J. Physiol. 532 (2001) 759–769, https://doi.org/10.1111/j.1469-7793.2001.0759e.x.
[70] R. Nandigama, M. Padmasekar, M. Wartenberg, H. Sauer, Feed forward cycle of hypotonic stress-induced ATP release, purinergic receptor activation, and growth stimulation of prostate cancer cells, J. Biol. Chem. 281 (2006) 5686–5693, https://doi.org/10.1074/jbc.M510452200.
[71] M. Oike, C. Kimura, T. Koyama, M. Yoshikawa, Y. Ito, Hypotonic stress-induced dual ca 2+ responses in bovine aortic endothelial cells, Am. J. Phys. Heart Circ. Phys. 279 (2000) H630–H638, https://doi.org/10.1152/ajpheart.2000.279.2.H630.
[72] A. Hazama, T. Shimizu, Y. Ando-Akatsuka, S. Hayashi, S. Tanaka, E. Maeno, et al., Swelling-induced, Cftr-independent Atp release from a human epithelial cell line, J. Gen. Physiol. 114 (1999) 525–533, https://doi.org/10.1085/jgp.114.4.525.
[73] N. Ullrich, A. Caplanusi, B. Brône, D. Hermans, E. Larivière, B. Nilius, et al., Stimulation by caveolin-1 of the hypotonicity-induced release of taurine and ATP at basolateral, but not apical, membrane of Caco-2 cells, Am. J. Phys. Cell Phys. 290 (2006) C1287–C1296, https://doi.org/10.1152/ajpcell.00545.2005.
[74] A. Hubert, B. Cauliez, A. Chedeville, A. Husson, A. Lavoinne, Osmotic stress, a proinflammatory signal in Caco-2 cells, Biochimie 86 (2004) 533–541, https://doi.org/10.1016/j.biochi.2004.07.009.
[75] E.-M. Collnot, C. Baldes, U.F. Schaefer, K.J. Edgar, M.F. Wempe, C.-M. Lehr, Vitamin E TPGS P-glycoprotein inhibition mechanism: influence on conformational flexibility, intracellular ATP levels, and role of time and site of access, Mol. Pharm. 7 (2010) 642–651, https://doi.org/10.1021/mp900191s.
[76] R. Taha, E. Seidman, G. Mailhot, F. Boudreau, F.-P. Gendron, J.-F. Beaulieu, et al., Oxidative stress and mitochondrial functions in the intestinal Caco-2/15 cell line, PLoS One. 5 (2010), e11817, https://doi.org/10.1371/journal.pone.0011817.
[77] M.F. Leal Denis, H.A. Alvarez, N. Lauri, C.L. Alvarez, O. Chara, P.J. Schwarzbaum, Dynamic regulation of cell volume and extracellular ATP of human erythrocytes, PLoS One. 11 (2016), e0158305, https://doi.org/10.1371/journal.pone.0158305.
[78] D. Jung, A. Alshaikh, S. Ratakonda, M. Bashir, R. Amin, S. Jeon, et al., Adenosinergic signaling inhibits oxalate transport by human intestinal Caco2-BBE cells through the a 2B adenosine receptor, Am. J. Phys. Cell Phys. 315 (2018) C687–C698, https://doi.org/10.1152/ajpcell.00024.2017.
[79] S.P. Colgan, B. Fennimore, S.F. Ehrentraut, Adenosine and gastrointestinal inflammation, J. Mol. Med. 91 (2013) 157–164, https://doi.org/10.1007/s00109-012-0990-0.
[80] R.E. Bucheimer, J. Linden, Purinergic regulation of epithelial transport, J. Physiol. 555 (2004) 311–321, https://doi.org/10.1113/jphysiol.2003.056697.
[81] Pafundo, American Journal of Physiology-Regulatory, Integrative and Comparative Physiology. (2004), https://doi.org/10.1152/ajpregu.00199.2004.